



January 2018

Scale-Up Feasibility And Novel Method Of Separation Of Carbon From An Oxygen Carrier

Nicholas A. Dyrstad-Cincotta

Follow this and additional works at: <https://commons.und.edu/theses>

Recommended Citation

Dyrstad-Cincotta, Nicholas A., "Scale-Up Feasibility And Novel Method Of Separation Of Carbon From An Oxygen Carrier" (2018). *Theses and Dissertations*. 2404.
<https://commons.und.edu/theses/2404>

This Thesis is brought to you for free and open access by the Theses, Dissertations, and Senior Projects at UND Scholarly Commons. It has been accepted for inclusion in Theses and Dissertations by an authorized administrator of UND Scholarly Commons. For more information, please contact zeinebyousif@library.und.edu.

SCALE-UP FEASIBILITY AND NOVEL METHOD OF SEPARATION OF CARBON FROM
AN OXYGEN CARRIER

by

Nicholas Anthony Dyrstad-Cincotta
Bachelor of Science, University of North Dakota, 2018

A Thesis
Submitted to the Graduate Faculty

of the

University of North Dakota

In partial fulfillment of the requirements

for the degree of

Master of Science

Grand Forks, North Dakota
December
2018

Copyright Page:


This thesis, submitted by Nicholas Anthony Dyrstad-Cincotta in partial fulfillment of the requirements for the Master of Science Degree from the University of North Dakota, has been read by the Faculty Advisory Committee under whom the work has been done and is hereby approved.



Dr. Clement Tang



Dr. Michael Mann



Dr. Srivats Srinivasachar

This thesis is being submitted by the appointed advisory committee as having met all of the requirements of the School of Graduate Studies at the University of North Dakota and is hereby approved.



Dean of the School of Graduate Studies

Dec 5, 2018

Date

PERMISSION

Title Scale-Up Feasibility and Novel Method of Separation of Carbon from an Oxygen Carrier and Coal By-Products
Department Mechanical Engineering
Degree Master of Science

In presenting this thesis, in partial fulfillment of the requirements for a graduate degree from the University of North Dakota, I agree that the library of this University shall make it freely available for inspection. I further agree that permission for extensive copying for scholarly purposes may be granted by the professor who supervised my thesis work or, in her (or his) absence, by the Chairperson of the department or the dean of the School of Graduate Studies. It is understood that any copying or publication or other use of this thesis or part thereof for financial gain shall not be allowed without my written permission. It is also understood that due recognition shall be given to me and to the University of North Dakota in any scholarly use which may be made of any material in my thesis

Name: Nicholas Anthony Dyrstad-Cincotta

Date: **December 5th, 2018**

TABLE OF CONTENTS

LIST OF TERMS	V
LIST OF FIGURES	VI
LIST OF TABLES	VIII
ACKNOWLEDGEMENTS	IX
ABSTRACT	X
CHAPTER I	1
INTRODUCTION	1
<i>Chemical Looping Combustion (CLC) Process</i>	<i>1</i>
<i>Chemical Looping Combustion Key Challenges</i>	<i>3</i>
Discussion of Research Need Relative to Prior Work.....	<i>3</i>
<i>Oxygen Carriers (OC) In Chemical Looping Combustion (CLC) Systems</i>	<i>6</i>
<i>Fluidized Beds</i>	<i>10</i>
Geldart’s Classifications of Particles	<i>11</i>
Fluidization Regimes	<i>11</i>
Bubbling Fluidization	<i>14</i>
Fast Fluidization.....	<i>14</i>
Elutriation Beds	<i>15</i>
Fluidized Beds Application in Carbon Stripping.....	<i>16</i>
<i>Loop Seals</i>	<i>17</i>
<i>Previous Work</i>	<i>18</i>
Phase I - Lab-Scale Char Separation Unit	<i>19</i>
Phase II –A– 50 kg/hr Char Separation Unit Testing	<i>22</i>
<i>The Solution</i>	<i>24</i>
<i>Project Description</i>	<i>25</i>
<i>Project Objectives</i>	<i>28</i>
<i>Scope of this project</i>	<i>28</i>
CHAPTER II	30
EXPERIMENTAL DESIGN & APPROACH	30
<i>Residence Time Analysis</i>	<i>32</i>
<i>Large Char Separator Design</i>	<i>34</i>
The Distributor Plate.....	<i>35</i>
Fluidization Engineering Calculations.....	<i>37</i>
<i>Small Char Separator</i>	<i>41</i>

<i>Transportation Leg/Loop Seal</i>	45
<i>Hoppers</i>	48
<i>Mixing Process</i>	48
<i>Holding Structure</i>	49
<i>Electronics</i>	50
<i>Programming</i>	51
<i>Approach & Methodology</i>	53
Experimentally determining U_{mf}	53
Testing Procedure	53
Combustion testing	54
Method of sample collection.....	55
CHAPTER III	56
RESULTS & DISCUSSION	56
<i>94 Micron OC Separation Results</i>	57
<i>230 Micron OC Separation Results</i>	59
<i>Solid Flow-Rate (Scale) vs Separation</i>	61
CHAPTER IV	62
CONCLUSION	62
CHAPTER V	64
FUTURE WORK	64
<i>Planned Work</i>	64

LIST OF TERMS

Attrition: Tendency for particles to wear away from abrasion to reactor walls

Agglomeration: Tendency for particles to collect together and form clusters.

Bottoms: Char lean mixture that is cycled to the oxidizer

Carbon Capture Rate (CCR):

Char: Un-utilized fuel (carbon)

Char Fed: Starting feed concentration of the mixture of char

Chemical Looping Combustion (CLC): Combustion through CLC processes is split into separate reduction and oxidation reactions in multiple reactors. The metal oxide supplies oxygen for combustion and is reduced by the fuel in the fuel reactor, which is operated at elevated temperature.

Chemical-Looping Combustion with Oxygen Uncoupling (CLOU): A novel method to burn solid fuels in gas-phase oxygen without the need for an energy intensive air separation unit

Chemical Looping Reforming (CLR): are the operations that involve the use of gaseous carbonaceous feedstock in their conversion to syngas in the chemical looping scheme.

Circulating Fluidized Bed (CFB): is a developing technology for coal combustion to achieve lower emission of pollutants.

Large Char Separator (LCS): Used for low-velocity density based segregation of particles.

Oxide: A binary compound of oxygen with another element or group

Oxidizer: Air reactor which oxidizes the metal carrier/oxygen carrier using oxygen.

Oxygen Carrier (OC): A metal carrier that has an affinity for oxygen release and absorption.

Particle Size Distribution (PSD): The relative amount, typically by mass, of particles present according to size.

Reducer: Fuel reactor in where carbon is combusted using oxygen released from the oxygen carrier.

Removal Rate: Compares to the carbon weight in the tops, to carbon weight in the bottoms and char fed.

Small Char Separator (SCS): Used for high velocity, terminal velocity based segregation of particles.

Splits: Refers to the ratio of tops to bottoms.

Tops: Char rich mixture, segregated out from the separators, which is cycled back to the fuel reactor.

LIST OF FIGURES

FIGURE 1: IRON BASED OXIDATION-REDUCTION REACTION.....	2
FIGURE 2: CHEMICAL LOOPING COMBUSTION PROCESS SCHEMATIC.....	2
FIGURE 3: SENSITIVITY OF COE TO OC MAKEUP IN CLC [2].....	4
FIGURE 4: OXYGEN CONCENTRATION VS TEMPERATURE OF CUPRIC AND IRON BASED OXYGEN CARRIERS [21]	10
FIGURE 5: GELDART’S CLASSIFICATION OF PARTICLES [22].....	11
FIGURE 6: FLUIDIZATION REGIMES BY FUNCTION OF MINIMUM FLUIDIZATION [22].....	12
FIGURE 7: EXPERIMENTALLY DETERMINING MINIMUM FLUIDIZATION VELOCITY VIA PRESSURE DIFFERENTIAL AND OPERATING VELOCITY [22]	13
FIGURE 8: MODEL TO ACCOUNT FOR ENTRAINMENT AND ELUTRIATION FROM FLUIDIZED BED. [22]	16
FIGURE 9: SCHEMATIC OF NON-MECHANICAL SOLIDS RECYCLE DEVICES [23]	18
FIGURE 10: CARBON CAPTURE PERCENTAGE WITH CARBON STRIPPER VS WITHOUT CARBON STRIPPER (LEFT) CARBON CAPTURE AS A PERCENTAGE OF RESIDENCE TIME (RIGHT) [26]	19
FIGURE 11: TRADITIONAL FLUIDIZATION REGIME CONTROL TEST SHOWING CARBON MIXING BEHAVIOR (LEFT TO RIGHT)	20
FIGURE 12: CHAR SEPARATION TEST SHOWING CARBON SEGREGATING (LEFT TO RIGHT) WITH NO MIXING	21
FIGURE 13: 50KG/HR CHAR SEPARATION UNIT.....	22
FIGURE 14: LCS RESULTS FOR 50KG/HR TEST OF 0.5WT% CHAR/OC MIX.....	23
FIGURE 15: EB RESULTS FOR 50KG/HR TEST OF 0.5WT% CHAR/OC MIX	24
FIGURE 16: CHEMICAL LOOPING COMBUSTION PROCESS SHOWING CHAR SEPARATION.....	25
FIGURE 17: PIPING AND INSTRUMENTATION DIAGRAM.....	27
FIGURE 18: ORIGINAL CHAR SEPARATION CONFIGURATION (LEFT) RECONFIGURED CHAR SEPARATION UNIT (RIGHT)	30
FIGURE 19: CONSTRUCTED 500 KG/HR CHAR SEPARATOR.....	31
FIGURE 20: LARGE CHAR SEPARATOR.....	35
FIGURE 21: DISTRIBUTOR PLATE FOR LARGE CHAR SEPARATOR.....	36
FIGURE 24: SMALL CHAR SEPARATOR.....	42
FIGURE 25: LOOP SEAL FOR A CFB PROCESS, BASU ET AL [28].....	46
FIGURE 26: TRANSPORTATION LEG/ LOOP SEAL.....	46
FIGURE 25: TRANSPORT LEG 500 KG/HR FLOWRATES FOR FINE OC	47
FIGURE 26: TRANSPORT LEG 500 KG/HR FLOWRATES FOR COARSE OC.....	47
FIGURE 27: DOUBLE DUMP VALVE SYSTEM SET UP	48
FIGURE 30: ELECTRONIC PANEL	50
FIGURE 31: PCS FOR CHAR SEPARATION.....	51
FIGURE 32: CHAR SEPARATION - LABVIEW BLOCK DIAGRAM.....	52

FIGURE 33: CHAR LEFT ON TOP OF BED	55
FIGURE 32: EFFECT OF FLOW REGIME ON 94 μM OC – ALL REGIME A	57
FIGURE 33: POOR FLUIDIZATION REGIME (LEFT) VS OPTIMAL FLUIDIZATION REGIME (RIGHT) – 94 MICRON OC	58
FIGURE 34: EFFECT OF FLOW REGIME ON 230 μM OC	60

LIST OF TABLES

TABLE 1: SUMMARY OF PHASE I RESULTS	21
TABLE 2: LCS RESIDENCE TIMES BASED ON VARYING BED DISCHARGE HEIGHTS	33
TABLE 3: SCS RESIDENCE TIME	34
TABLE 4: REGRESSION VALUES FOR CALCULATING MINIMUM FLUIDIZATION VELOCITY	38
TABLE 5: REFERENCE VALUES FOR CALCULATIONS – 94 MICRON OC.....	38
TABLE 6: REFERENCE VALUES FOR CALCULATIONS - 230 MICRON OC	39
TABLE 7: DISTRIBUTOR PLATE CALCULATION VARIABLES	40
TABLE 8: SEPARATION CUT POINT VELOCITY EQUATION VARIABLES – 94 MICRON OC.....	44
TABLE 9: SEPARATION CUT POINT VELOCITY EQUATION VARIABLES – 230 MICRON OC	44
TABLE 10: EXPERIMENTALLY OBTAINED OPTIMAL BED VELOCITIES FOR 94 TO 230 MICRON PARTICLE SIZES	56
TABLE 11: SEPARATION RESULTS AND OPERATING VELOCITIES AT VARYING SCALE AND PROCESS CONDITIONS.....	61

ACKNOWLEDGEMENTS

I wish to express my sincere appreciation to the members of my advisory committee for their guidance and support during my time in the master's program at the University of North Dakota. I would like to thank my senior design team, Brent Peterson and Jordan Sperl, for helping to set the foundation for this project. I would also like to thank the Institute for Energy Studies and all that they have done for me; without this department I would not be in the position I am today, nor would I have been given the opportunity to work on a project like this. I am grateful for Dr. Srivats Srinivasachar for his guidance and challenging me to think in ways I've never thought before. I am additionally grateful for Junior Nasah for all of his intellectual contributions and ensuring I keep on task. He ensured that everything I did would add value to this project. I extend my deepest gratitude to Harry Feilen, who taught me all the skills I needed to know in order to complete a project of this magnitude. Without his time and guidance, this project would not have reached fruition as it did.

ABSTRACT

This project targets the development of a technology for segregating fuel-based contaminants (char/carbon) from oxygen carrier material in the context of chemical looping combustion applications. In chemical looping, the well-mixed solids that flow from the fuel reactor consisting of char, ash, and oxygen carrier particles cannot be completely separated into their constituents before they enter the air reactor. The slip of carbon leads to char oxidation in the wrong reactor and poor carbon dioxide separation efficiency. The buildup of ash that is not rejected necessitates rejection of larger quantities of oxygen carrier material, resulting in a high operating cost penalty. An efficient method to separate char from oxygen carrier material is critical for the deployment of chemical looping technology.

This project developed a novel method for char separation from oxygen carrier that is specifically tailored to chemical looping combustion and its unique constraints and process conditions. The segregation system consists of a novel combination of methodologies that together provide very high segregation efficiency, even under the extreme conditions of chemical looping systems. Following the successful demonstration in Phase I at the lab-scale, this Phase II project involved a significant scale-up. The components in the novel segregation system were optimized through parametric evaluation of several process conditions. Design emphasis was on reducing equipment size and energy input. There is a target of 80% removal of char in the exit stream of oxygen carrier. Due to the scale of the project, tests were completed under cold flow conditions, meaning room temperature.

CHAPTER I

INTRODUCTION

There has been a significant amount of information redacted from this report to protect confidentiality and proprietary rights. This may leave the reader with some questions which cannot be disclosed at this time.

Chemical Looping Combustion (CLC) Process

Carbon neutral energy represents one of the more pressing technical challenges of this century and will no doubt play a major role in issues such as the global climate change, international politics, and commerce in the future. Increased dependency on advanced low-emission energy technologies and improvements with the energy efficiency of existing fossil-fuel-based power generation assets are crucial for a carbon free energy future.

Chemical Looping Combustion (CLC) is one of several developing technology options capable of advancing low-emission energy technologies and helping in a various range of applications for productions of fuels, chemicals, and electricity. CLC makes use of an oxidation-reduction reaction in order to convert coal/carbon into energy. An example of the oxidation-reduction reactions for an iron-based material is shown in Figure 1. In the oxidation stage, the iron oxygen carrier Fe_3O_4 gains an oxygen molecule and becomes Fe_2O_3 . This extra oxygen molecule from the Fe_2O_3 is used towards ignition of the char in the fuel reactor. It is in this fuel reactor where the iron-based material releases that oxygen molecule, thereby returning to its reduced state. The net reaction forms CO_2 and H_2O , both of which can be controlled and captured.

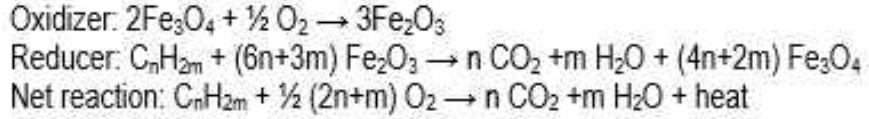


Figure 1: Iron based oxidation-reduction reaction

A simplified oxidation-reduction process schematic is found in Figure 2.

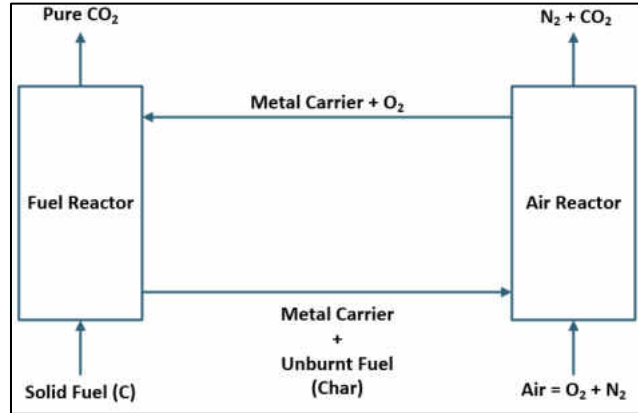


Figure 2: Chemical looping combustion process schematic

Chemical looping processes can be designed in such a manner that the energy and exergy losses of the overall process are minimized, while allowing for the separation of the undesired products (e.g., CO_2) produced from the reactions to be easily accomplished. This allows the process to yield an overall efficient, economical, and low-emission process. For example, if chemical looping is applied as a combustion process, fuel combustion would take place in the absence of nitrogen, ensuring that the main components of the flue gas are CO_2 and H_2O , which can be easily separated from CO_2 by cooling the exhaust gas and removing the condensed liquid water. Thus, fuel and air never mix, and CO_2 does not become diluted by nitrogen. This means there is typically no or little energy penalty associated with the capture of CO_2 when chemical looping combustion (CLC) is employed. Two of the main issues currently limiting applications of CO_2 capture options are dilute CO_2 streams when treated with solvents, such as amines, require substantial energy for regeneration for gas-liquid applications, and for solid-gas applications, non-utilized fuel (carbon) that reaches the air reactor. Overall, it is this ability for the separation of

undesired products, such as CO₂, which makes the chemical looping process a valuable tool in low-emission technologies.

Furthermore, the ability to incorporate a diverse range of intermediates provides chemical looping with versatility, allowing it to be used in a wide range of applications. For example 1) chemical looping gasification (pre-combustion capture of CO₂); 2) chemical looping reforming (CLR; pre-combustion capture of CO₂); 3) CLC (in situ capture of CO₂); 4) sorbent chemical looping for post combustion capture of CO₂; 5) chemical looping air separation for oxygen supply in oxy-fuel and integrated gasification combined cycle (IGCC) operations; and 6) chemical looping removal of ventilation air methane (VAM) in mining processes [1].

Chemical looping processes for condensed phase reactants (e.g., solid or liquid fuels) cannot proceed unless either the condensed phase reactants are converted into the gas phase for subsequent gas/solid reactions at the surface of solid intermediates (SI) particles or, instead, when the SIs release their active ingredients (e.g., O₂) into the gas phase for subsequent gas/solid reactions at the surface of the condensed-phase reactant. Because of the technical difficulties associated with both approaches, the early CLC-based systems for power generation were mainly designed for gaseous fuel feedstock. However, it was recognized very early that the greater acceptance of the CLC relies on extending the concept to fossil and organic based solid fuels, in particular, coal. Such improvements are specially considered to be important in the context of carbon capture and storage (CCS) because of the ability of CLC for CO₂ separation/ capture.

Chemical Looping Combustion Key Challenges

Discussion of Research Need Relative to Prior Work

Chemical Looping Combustion (CLC) has emerged as an attractive alternative for CO₂ capture, where a near-pure CO₂ stream is produced from fossil fuel combustion without the use of

oxygen obtained from air separation. In this type of system, a solid oxygen carrier (OC) is used to bring oxygen to the fuel and convert it to stream of CO₂ and H₂O. In this process, the OC is reduced. The solid is then regenerated (oxidized) separately using air. CLC technology is expected to be more cost-effective and energy efficient compared to oxygen separation from air by other processes and to supply nitrogen-free oxygen for fuel conversion. With the possibility of governments imposing a carbon tax, demand for developing CO₂ capture technologies like CLC is becoming increasingly popular.

Stevens et al. (2014) summarize the key technical challenges related to the development of CLC [2]. One challenge is the high cost of electricity (COE) for CLC which is a direct result of the high unit costs of the OC make-up (Figure 3). Development of lower cost OC (~\$0.05/lb) through identification of low-cost raw materials and alternate processing is essential for bringing down the COE.

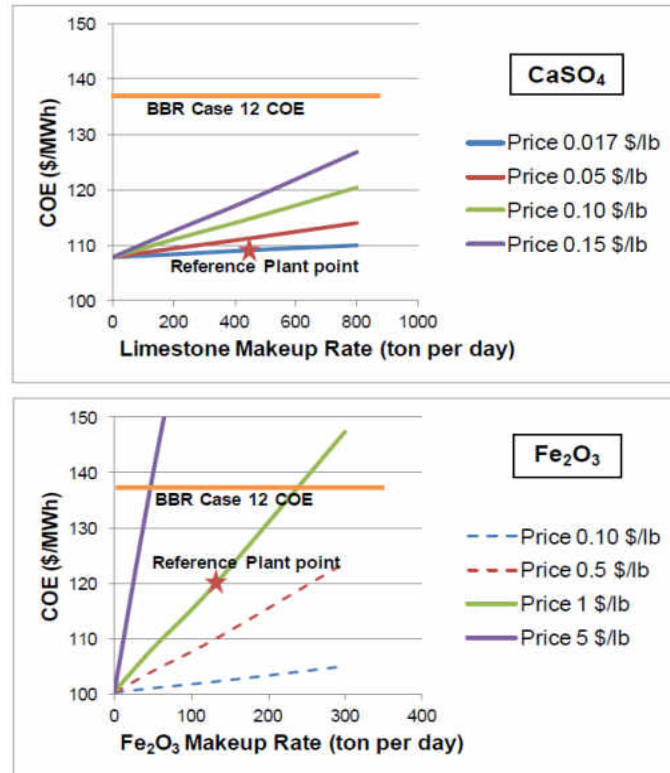


Figure 3: Sensitivity of COE to OC makeup in CLC [2]

In addition to the low cost and wide availability, the OC must have: 1) high reactivity with fuel and oxygen and resistance to sulfur poisoning; 2) low fragmentation and attrition and a low tendency for agglomeration/sintering; 3) low risk for health and safety; and 4) sufficient oxygen transfer capacity. Lyngfelt (2015) identified a structured approach to OC development comprising sequential screening and selection using laboratory-scale fluid bed reactivity and attrition testing followed by testing in larger units with relevant velocities and contacting; such an approach is taken in the proposed project [3].

A second key challenge for CLC is that reducer char gasification rates are limiting because of the low temperature operation and inherent low rate of carbon gasification at CLC conditions. Novel gas-solid contacting methods which can provide counter-current contacting using OC particle sizes relevant to fluidized bed operation (as opposed to moving bed) along with novel carbon stripping methods will be necessary to maintain scale-up possibility, meet the carbon capture requirement, and minimize oxygen demand for reducer off-gas (unconverted H₂, CO). Stevens et al. (2014) also identified that a carbon stripping system was essential, but has the challenge of processing large amount of solids (~10,000 tons/h for a 500 MW_e plant) and having less than one percent carbon and to extract about eighty percent of carbon while minimizing the recirculation of deactivated (reduced) OC to the reducer [2].

When a solid fuel is used, only a portion of the fuel is converted in a single pass in the fuel reactor. This necessitates the need for segregation of the material leaving the fuel reactor into unconverted fuel (char) and OC, performed by a char separator. The separated char can be returned to the fuel reactor to increase its conversion. If unconverted fuel is transferred to the air reactor, it would be combusted in air releasing its CO₂ with the N₂-rich gases. Since the primary motivation of chemical looping technology is to achieve a high carbon capture rate (CCR), an efficient char

separator is mandatory. The CCR is the percent of fuel carbon that is converted to CO₂ in the fuel reactor. The design and development of such a char separation device is the object of this research project.

Char separation is a critical process step in chemical looping combustion of solid fuels. The oxygen carrier (OC) is the most important component of a CLC system. Suitable OCs for solid fuels in the CLC process must have selectivity to form CO₂ and H₂O, high oxygen transport capacity, reactivity and attrition resistance, be environmentally benign, and have negligible agglomeration and reaction tendency with coal ash. A literature research review of oxygen carriers suitable for use with solid fuels is available in the following section.

Oxygen Carriers (OC) In Chemical Looping Combustion (CLC) Systems

Copper-Based Materials

Cu-based materials have shown to be very reactive, with full combustion of gasification products at a mass ratio of OC/solid fuel of only 10:1 at 850 °C [4]. Cu-based oxygen carriers are especially suited for the chemical looping oxygen uncoupling (CLOU) process, where oxygen is released from the carrier in the fuel reactor. Cu-oxygen carriers prepared by impregnation on SiO₂, TiO₂, γ -alumina or co-precipitation with alumina [5] have excellent chemical stability and mechanical strength after multi-cycle testing. Other supports have shown unacceptable levels of attrition. The main concern with Cu-based oxygen carriers is agglomeration at temperatures exceeding 800°C in the fuel reactor due to melting. A content of less than 20% CuO was required to avoid agglomeration issues. Forero et al. [6] analyzed the behavior of a Cu-based oxygen-carrier with γ -Al₂O₃. Stable operation for more than 60 h was only feasible below 800 °C in the fuel reactor and 900 °C in the air reactor.

Adánez et al. [7] prepared stable bimetallic Cu-Ni/O₃ particles and observed that the presence of NiO in the oxygen carrier stabilized the CuO phase. Long-term tests in a CLC unit under continuous operation showed high metal oxide utilization, and low and stable attrition rate after 67 h of operation at high temperature. This was the first time that a Cu-based oxygen-carrier, prepared by a commercial manufacturing method, exhibited good behavior at these temperatures.

The required inventory of Cu-oxygen carrier is significantly lower (120-200 kg/MWth) compared to other OCs (e.g. Fe-based OC-2000 kg/MWth). Even with a lower inventory requirement, the significantly higher cost implies that it needs to have high particle lifetimes and excellent attrition resistance. Density of the Cu-based OC ranged from 3700-5400 kg/m³.

Iron-Based Materials

Iron-based materials represent an abundant, low cost, environmentally benign alternative for OC material, but have much lower reactivity and consequently a high OC to solid fuel ratio (50-100:1). At Ohio State University [8], the iron-based OC developed incorporates inert support materials, increasing the reactivity and recyclability. A 200-hour test performed in a 25 kWth chemical looping facility with lignite and sub-bituminous coal was presented by Bayham et al. [9], and showed minimal CH₄ /CO/H₂ slippage through the fuel reactor. Particle size of the oxygen carrier was around 1.5-5 mm, the fuel reactor was operated as a moving bed and the air reactor as a fluidized bed. Other researchers have used Fe-based carriers, including Leion et al [10]. An OC of 60 wt.% Fe₂O₃ and MgO₄ as inert was used with petroleum coke as the fuel. High reactivity was found with the gasification products (H₂ and CO) of coke with steam. Shen et al [11] used a biomass fuel in a continuous 10 kWth CLC system and accomplished a 30 h test. The fuel reactor

temperature was varied between 740 and 920°C and CO₂ was used as a gasification medium. Low reactivity of the oxygen carrier was observed due to sintering.

The use of cheap natural minerals such as ilmenite (iron titanate) represents another promising OC candidate. Berguerand and Lyngfelt [12], [13] operated a 10 kWth unit using coal and petroleum coke; combustion efficiencies of 85-95% were obtained. Thon et al. [14] used ilmenite in the size range of 100-400 microns. The solid fuel was lignite with 70 percent smaller than 150 microns. Activated ilmenite (after circulating in reactor system) was determined to have a density of about 3600 kg/m³ [15]. Results also showed a low tendency for attrition and agglomeration for this material and its low market price makes it a promising option for use as an oxygen carrier.

Calcium-Based Materials

GE Power (formerly Alstom) is developing a CLC process where CaSO₄ is used as oxygen-carrier for heat generation, syngas production or hydrogen generation [16]. For their 3 MWth prototype CLC unit, combustion efficiencies of 95-97% were achieved. Density of CaSO₄ is around 2600 kg/m³. The size of the OC used is comparable to bed ash from a circulating fluid bed combustor, with the coal being finer.

Manganese-Based Materials

Although a promising metal oxide, Mn-based oxygen carriers have not been widely tested so far. The disadvantage of manganese oxides is their incompatibility with common support materials like Al₂O₃ and SiO₂. Mn-based OC supported on ZrO₂ stabilized with MgO has shown good reactivity with syngas components [17], but lower reactivity has been found for CH₄ [18]. These particles have also been tested in a continuously operated 300Wth CLC unit [19]. Absence

of agglomeration and low attrition rate were observed. Very high efficiencies (>99.9 %) were obtained at temperatures in the range 800-950 °C for syngas combustion.

Arjmand et al. [20] evaluated the CLC performance of various manganese ores with two fuels, petroleum coke and a wood char. The particle size of the OC was 150-350 microns and activated densities ranged from 2200-3600kg/m³. Fuel particles used were 180-250 microns, similar in size to the OC.

Attrition and Its Impacts on Char/Oxygen Carrier Separation

The attrition behavior of OCs is an important characteristic for char/ash separation as the particle size distribution of the fresh OC is only partly relevant for an operating system. Because of attrition, the size of the circulating OC will be finer than the fresh material. This reduces differences in the terminal velocity values for the char and the OC, making efficient separation more difficult. All OCs have a limited lifetime, either because of reactivity loss, or due to attrition processes that elutriate the OC particles out of the system. Attrition influences two important aspects of fluid bed operation, namely particle elutriation and PSD. Elutriation of fine particles out of the system, mainly caused by the surface abrasion mechanism, may lead to the loss of bed material from the reactors. On the other hand, a significant change in the PSD of the bed material due to fragmentation affects the operation of the fluidized bed unit. In fact, bed fluid-dynamics, heat and mass transfer coefficients, and heterogeneous reaction rates depend on the PSD of the bed material [20].

Temperatures Effect on Oxygen Concentration in Oxygen Carriers

The temperature where oxidation/reduction readily occurs for each of the mentioned oxygen carriers is a critical factor in determining if the material is viable for use in a chemical looping combustion system. A good oxygen carrier should have an equilibrium pressure of oxygen

below 4% at temperatures of 800 to 1000 °C. A material that fits this criteria means that oxide has good oxygen affinity, which allows for oxidation. The cupric based oxygen carriers oxidize and reduce at lower temperatures, while iron based oxygen carriers start to oxidize and reduce at higher temperatures. Figure 4 shows the variation of oxygen levels of the two oxygen carriers based on temperature.

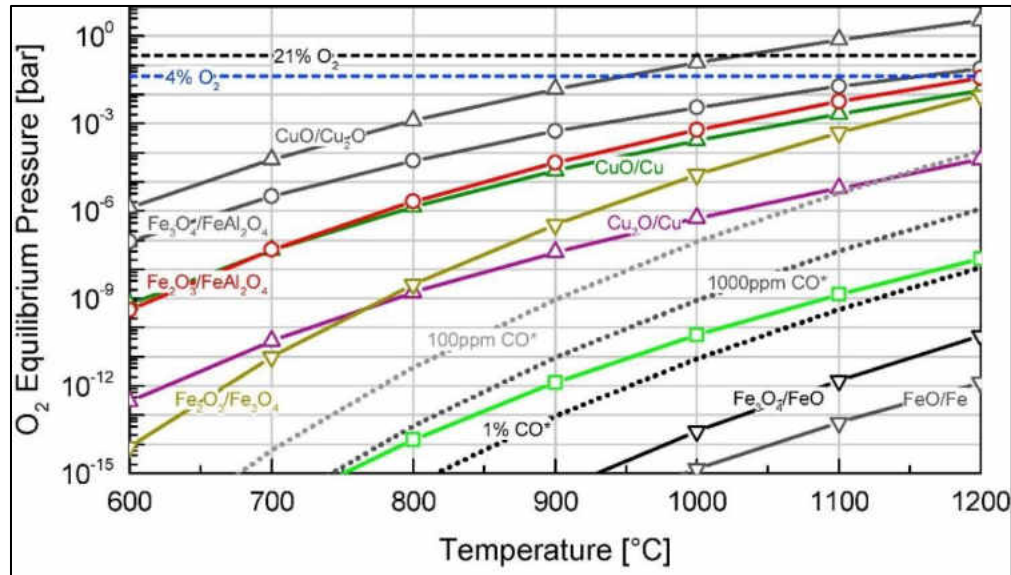


Figure 4: Oxygen Concentration vs Temperature of Cupric and Iron based oxygen carriers [21]

Depending on the application, lower temperatures may be required making a copper based oxygen carrier ideal. For example, the rate at which the oxygen is released could also be important to ensure that the kinetics are fast enough to get reactions to occur in reasonable time.

Fluidized Beds

Fluidization processes have gained in popularity and received greater attention for a wide range of chemical and physical operations. Liquid-solid and gas-solid fluidization systems possess a multitude of characteristics in common but they behave quite differently. For example, the increase in flow rate above minimum fluidization usually results in a smooth expansion of the liquid-solid bed. For the gas-solid systems an increase of the flow rate beyond minimum fluidization results in large instabilities with bubbling and channeling of gas observed. These

fluidization principles can be applied to carbon stripping technologies and assist in reduction of carbon in CLC systems.

Geldart's Classifications of Particles

Solids with different particle characteristics show different fluidization behaviors. According to Geldart (1972), powders can be classified into four groups A, B, C and D based on their average size, density, and their fluidization properties. Groups A, B, and D follow the general fluidization regimes, while Group C particles are highly cohesive and hence cannot be subjected to normal fluidization. Figure 5 represents Geldart's classification of particles, expressed in terms of particle diameter and $\rho_s - \rho_g$ (solid density – fluidization gas density).

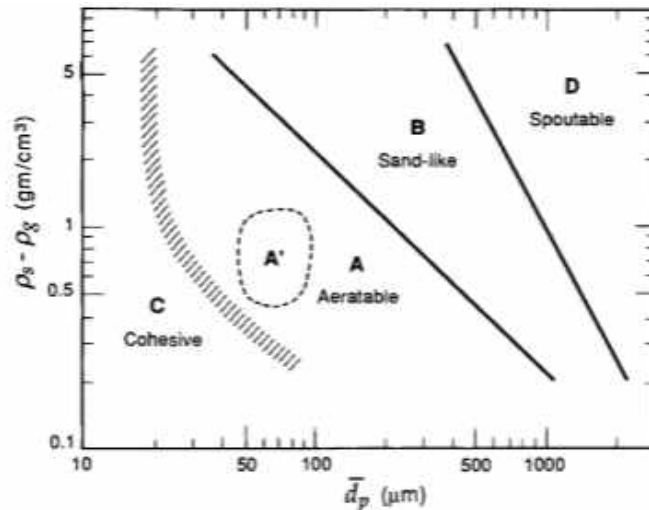


Figure 5: Geldart's Classification of Particles [22]

Fluidization Regimes

When gas is introduced at the bottom of a bed containing solid particles at a very low flow rate, the gas passes through the voids between the stationary particles without moving the particles. This is termed a fixed bed regime because the bed does not expand. In increasing the superficial gas velocity, U_g , the voids between particles become larger and particles start moving and oscillating until they become totally suspended. At this point the drag exerted on the particles by an upward flowing gas balances the weight of the particles making the solid particles suspended.

The superficial gas velocity at which this occurs is called the minimum fluidization velocity U_{mf} . With an increase of the superficial gas velocity, more fluidization regimes can be observed: namely, bubbling, slugging, turbulent and fast fluidization. Figure 6 below represents a visualization of the progression of fluidization regimes as a function of minimum fluidization.

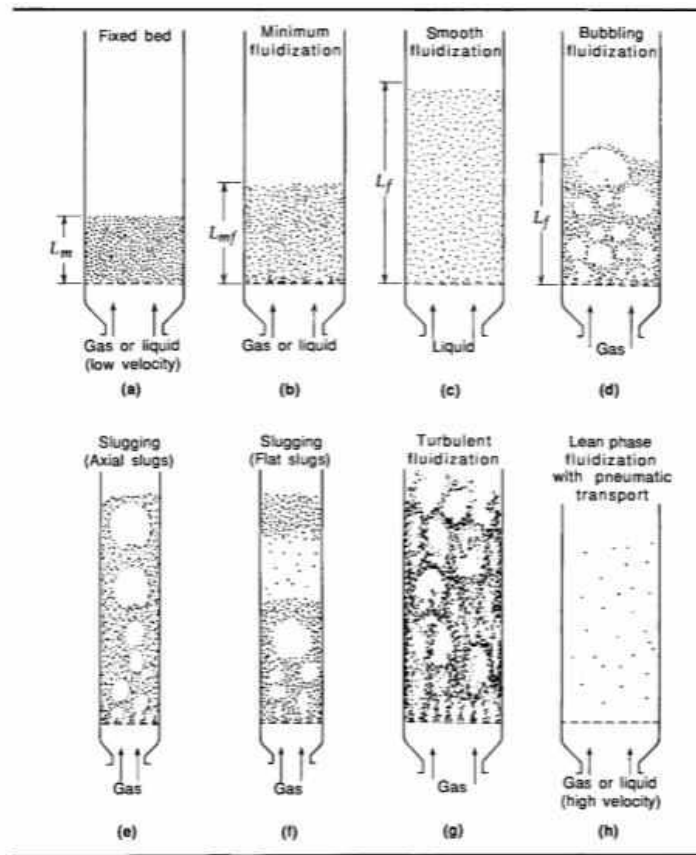


Figure 6: Fluidization Regimes by function of minimum fluidization [22]

The point at which flow causes the bed of particles to expand and lift into the vertical bed is marked by a simple balance. At minimum fluidization (U_{mf}), drag force (F_d) balances with the gravitational force (F_g) there is a minimal to no change in pressure drop.

$$0 = F_g + F_d \quad (1)$$

The net gravitational forces on the bed of particles must consider the weight (W) of the particles and the buoyancy forces (F_b).

$$F_g = W - F_b \quad (2)$$

$$F_g = (\rho_p - \rho_f)g V_p \quad (3)$$

Where ρ_p is the density of the particles, ρ_f is the density of the fluid, g is the gravitational acceleration constant, and V_p is the total volume of particles within the fluidized bed.

Graphing the differential pressure (ΔP) versus operating velocity (U_o) can be used to help find the experimental minimum fluidization velocity of the bed. Where the U_{mf} can essentially be determined as the intersection point where the pressure levels off meets the operational velocity. The operational velocity is set to match the project objectives. For a bubbling bed operation, a lower operational velocity is required, compared to a circulating bed which requires higher operational velocities.

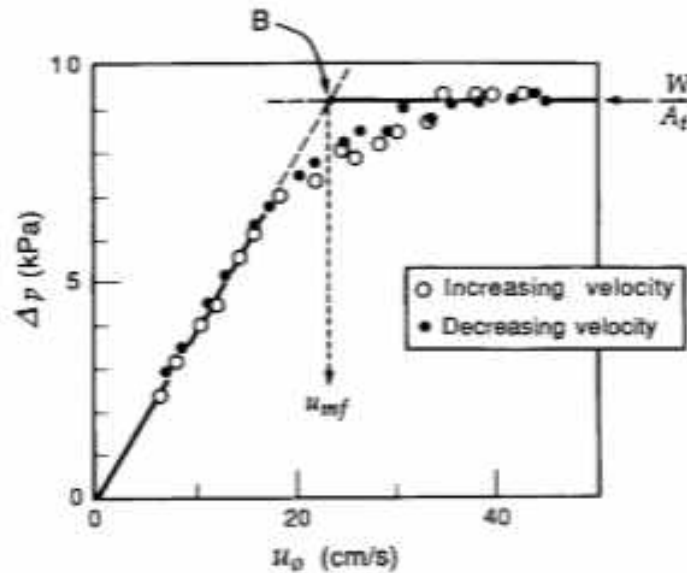


Figure 7: Experimentally determining minimum fluidization velocity via pressure differential and operating velocity [22]

Figure 7 represents the experimental means of verifying the minimum fluidization velocity. The U_{mf} is dependent on the density and particle size of a material and may vary as testing progresses. Thus as the particles attrite or agglomerate, the U_{mf} will be affected.

Bubbling Fluidization

The clearest difference between this and the other two regimes is the existence of large bubbles and a clearly outlined free surface. The bed is very nonhomogeneous due to the presence of the bubbles and the pressure drop across the bed changes in time. As the fluidization velocity increases, large bubbles break up into several smaller ones. When the bubbles burst at the bed surface two processes take place; 1) the surface gas velocity can be much higher than the mean fluidization velocity, so the larger particles can also be thrown out far from the bed surface; 2) only particles with low free fall velocity lower than that of the gas velocity will be elutriated far from the bed surface. Particles of greater size return (fall back) into the bed, but lots of smaller particles can be carried away from the bed by the flowing gas. For that reason, the fluidized bed surface is very disturbed and there is no sudden change in particle concentration. When the break-up process overcomes the merging of the bubbles, fluctuations of the pressure drop become smaller. This is the moment when turbulent regime occurs, with no big bubbles in the bed.

Fast Fluidization

With an increase of the flow rate beyond minimum fluidization, large instabilities with bubbling and channeling of gas are observed forming the bubbling fluidization regime. In smaller diameter beds, as the bubbles rise in the bed they coalesce and grow while particles flow down the wall around the rising void of gas creating what is known as a slugging regime. At higher gas velocities the terminal velocity of the solid is exceeded and the solid entrainment becomes noticeable, thus instead of the creation of bubbles, a turbulent motion of solid clusters are observed forming a fast fluidization bed.

Terminal velocity is the steady speed achieved by an object freely falling through a gas or liquid. Terminal velocity is achieved when the speed of a moving object is no longer increasing or decreasing; the object's acceleration (or deceleration) is zero. The force of gas resistance is fairly

proportional to the speed of the falling object, so that gas resistance increases for an object that is accelerating, having been dropped from rest until terminal velocity is reached. At terminal velocity, the gas resistance equals in magnitude the weight of the falling object. Because the two are oppositely directed forces, the total force on the object is zero, and the speed of the object has become constant. Terminal velocity is reached when the drag force due to moving through air is equal (but opposite) to the gravitational force. Now, the gravitational force is proportional to the density, while the drag force has nothing to do with density, but everything to do with how large the particle is. Assuming the particle is spherical, as the diameter and density increases, the terminal velocity should increase.

Elutriation Beds

The section between the dense bed and the exiting gas stream is referred to as the freeboard. The function of the freeboard is to allow solids to separate from the gas stream. As the freeboard height increases the entrainment lessens. At a certain point a freeboard height is reached above which entrainment becomes nearly constant. This is called the transport disengaging height (TDH). As bubbles rise and burst they carry solids into the freeboard. This can be particles large enough that they are below the terminal velocity. These particles will disengage and fall back into the bed. Fine particles, which are above the terminal velocity, will not disengage and will be carried out of the bed. This is known as elutriation, i.e. the selective removal of fines by entrainment from a bed consisting of a mixture of particle sizes. Elutriation can happen both above and below the TDH.

Figure 8 represent a model that accounts for the varying aspects of entrainment inside a dense bubbling bed. From the dense bed, there is pneumatically transported completely dispersed solids, travelling at velocity u_1 . The second phase is projected agglomerates moving upward with

velocity u_2 . The third phase is descending and groups of thick dispersion moving downward with velocity u_3 .

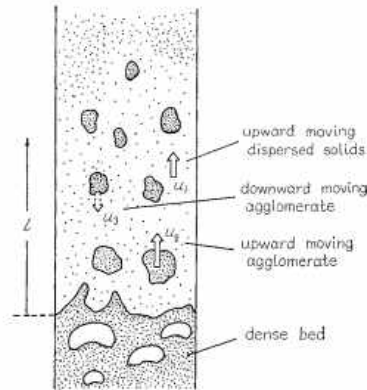


Figure 8: Model to account for entrainment and elutriation from fluidized bed. [22]

According to Levenspiel [22], at any level in the bed the rate of dissipation of agglomerates to form dispersed solids of the first phase is proportional to the concentration of agglomerates of solids at that level. Additionally, upward moving agglomerates occasionally reverse direction and move downward. In this case, agglomerates are defined as a cluster of independent suspended particles. This is different than agglomerate, which is defined as the sintering of particles together to form a larger, agglomerated particle.

Fluidized Beds Application in Carbon Stripping

Following the fluidization regimes listed in Figure 6, as minimum fluidization is increased, particles behave differently between phases. In terms of gas-solids fluidization, traditional fluidization regimes at lower minimum fluidization velocities promote mixing of the particles in the bed. However, at higher velocities, particles are transported out of the bed. The transport out of the bed occurs as particles reach their transport velocity, which is a function of both particle size and density. Traditional carbon stripping technologies make use of the transportation phase, which goes off the principle of separation via particle-size. These technologies, primarily denoted as Elutriation Beds (EB), separate particles based on their terminal velocity. Since EB do not take

into consideration the density difference, along with crossing of the particle size distribution between the two solids, they involve mixing of particles and are not as efficient as they could be. By applying a novel approach to the fluidization regime and controlling the flowrates based on minimum fluidization velocities, the separation efficiency could be increased greatly. Any increase in the separation efficiency or reduction in required energy input (by operating at lower velocities) would help validate this technology for use in CLC systems. Under this project, scale-up feasibility of such a carbon stripper will be investigated.

Loop Seals

The transportation of solids can be a very challenging task, especially when high temperatures and pressures are involved. Loop seals are an attractive an attractive option for chemical looping combustion because they consist of no moving parts and maintain a gas seal between components. This helps them to operate under harsher conditions.

Loop seals have also been referred to as solid recycle systems and non-mechanical valves, which are devices that assist with the flow of solids without any mechanical force. Air or a desired gas is used for the movement of solids through these valves. With enough aeration (fluidization gas), the solid particles behave as a fluid. As flow of aeration gas is increased, the gas carries the solids through the valve. Varying the aeration flow allows the mass flow rate of the particles to be more easily controlled. There is a threshold amount of gas supply which must be added before solids begin to flow. The performance of loop seals have been found to be dependent on operating pressures. Depending upon the pressure balance, which the weight of the solids help establish, the gas sometimes move up in opposite direction. Figure 9 shows the most common loop seal designs used in CLC and Circulating Fluidize Bed (CFB) systems.

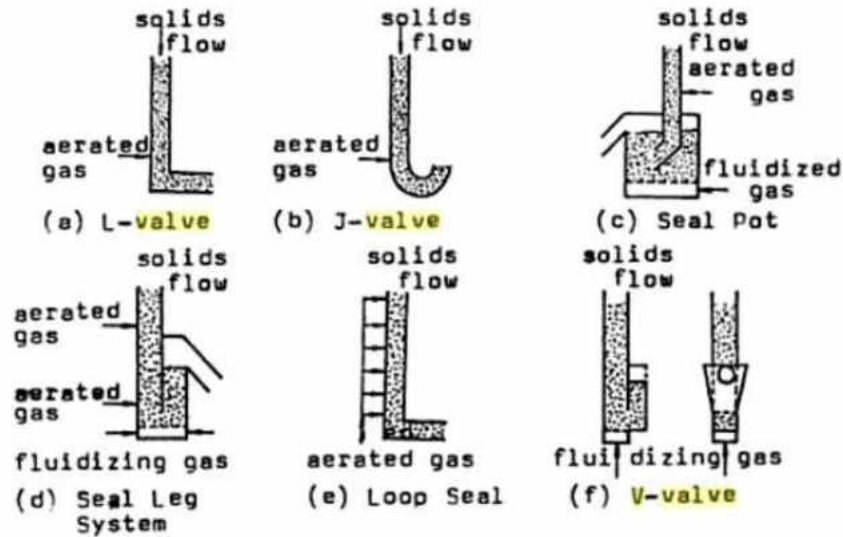


Figure 9: Schematic of Non-mechanical Solids Recycle Devices [23]

The three most common loop seals are the L-valve, V-Valve, and J-Valve. Information on these loop seals is limited and they are one of the least understood aspects of a CLC or CFB system, despite being critical to the operation of such a system. The main challenges that come with operation of a loop seal are design size, particle size, and the pressure balance of the system. Designing a loop seal too small might not allow for adequate flow of solids and designing it too large would require a large volume of air. These non-mechanical valves work well with Geldart's group B and D particles for sizes above 100 microns [25]. Consistent mass flow rates depend heavily on consistent pressures. Solids in the non-mechanical valves are moving in a packed-bed condition. This means the pressure drop through the valve will rise if the relative velocity between the solids and gas is increased. The pressure drop will rise until it is equal to the weight of solids in the valve. At this point is when the movement and resulting transfer of solids occurs. This is typically when minimum fluidization conditions have been met.

Previous Work

Carbon stripping technologies are a critical process step in chemical looping combustion of solid fuels. In CLC reactors, the carbon is not completely consumed, and as a result well-

mixed solids consisting of char, ash, and oxygen carrier flow from the fuel reactor. This slippage of carbon from the reducing reactor will lead to char oxidation in the oxidation reactor. The subsequent production and release of CO₂ causes a carbon capture penalty. According to models created by Kramp et al, depending on the choice of fuel, CO₂ capture rates can increase by nearly 40% when a carbon stripping technology is implemented into the process [26]. Trials were also conducted using extended residence times in attempt to increase the carbon capture rate of a CLC system without carbon stripping technologies.

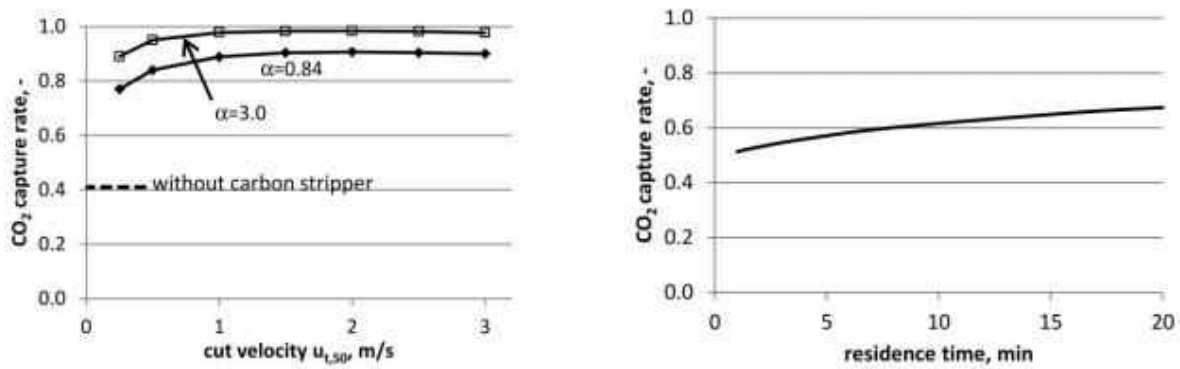


Figure 10: Carbon capture percentage with carbon stripper vs without carbon stripper (Left) Carbon capture as a percentage of residence time (Right) [26]

As shown in Figure 10, even with an increase in residence time to allow for additional capture of CO₂, the carbon capture rate was unable to match that of a CLC system with an attached carbon stripper.

Phase I - Lab-Scale Char Separation Unit

The University of North Dakota Institute for Energy Studies was awarded a Phase I char separation project at the in 2014. In this project, they applied principles of fluidized beds with novel flow regimes to carbon stripping technologies in an attempt to demonstrate the novel application could separate char with-in solid-gas CLC processes. The experimental set-up included an Elutriation Bed, also referred to as the Small Char Separator (SCS), for separation via terminal velocity of the char particles, as well as a Large Char Separator (LCS), which was used for density-

based separation of the char from the oxygen carrier. In these tests, batch systems were constructed for the proof-of-concept of the carbon stripping technology. The tests used glass beads and carbon (activated carbon) as a test medium. It was envisioned that the char laden OC would first undergo primary separation in the LCS, with the OC then moving to the EB to remove additional char.

To show the differences between mixing in a fluidized bed and the LCS which promotes separation, two tests were conducted for comparison purposes. In each test, the starting conditions were a layer of oxygen carrier, beneath a layer of char, beneath a layer of the two mixed together. Testing for each of the two experiments was done using a circular fluidized area design. Figure 11 represents a visual test using a traditional bubbling fluidized bed regime, which was used as a control. In this control test, there is significant back-mixing of the carbon with the oxygen carrier. Rather than separating into their appropriate layers, the carbon and oxygen carrier dispersed homogeneously throughout the bed.



Figure 11: Traditional fluidization regime control test showing carbon mixing behavior (left to right)

In the LCS test, a novel approach to fluidization regimes was attempted. As shown in Figure 12, there was good separation of carbon with no back mixing. A substantial amount of carbon made its way to the top of the fluidized bed, with minimal amounts of carbon making its way to the bottom of the bed.

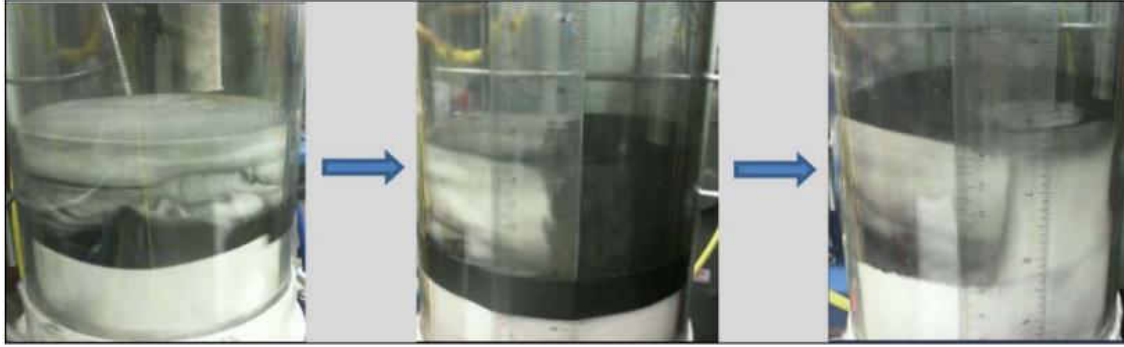


Figure 12: Char Separation test showing carbon segregating (left to right) with no mixing

Testing with the EB alone was performed to establish a baseline char separation for comparison to the combined EB and LCS. When using a fluidization velocity of 30 cm/s in the EB (to minimize OC elutriation), 48% of carbon was removed with 5% elutriation of the glass beads. Using GE pilot OC/char combination, 58% separation was achieved with 19% elutriate. For the EB, it was revealed that greater than 45% carbon will result in 15% of more OC being segregated with the carbon. Additional tests were conducted with the LCS and EB in tandem. Results of Phase I are presented in Table 1 below.

Table 1: Summary of Phase I Results

Size Fraction	Carbon Removed	OC Carried Over
EB Performance		
> 105 μm	35%	6%
< 105 μm	67%	41%
Total	58%	19%
Combined EB+LCS Performance		
> 105 μm	64%	17%
< 105 μm	80%	49%
Total	71%	29%

This proof-of-concept testing showed that use of an EB alone is not suitable for segregating the char from OC. Placement of the LCS upstream of the EB will help reduce operating velocities in the EB and minimize OC entrainment. Use of the EB+LCS combination yielded 71% separation

with only 29% elutriation. These results gave sufficient evidence that this char separation approach is feasible method of carbon stripping.

Phase II –A– 50 kg/hr Char Separation Unit Testing

The success of Phase I lead to a Phase II continuous flow (50 kg/hr) char separation cold flow unit was constructed and tested. This unit consisted of a holding vessel, LCS, and an EB, with transportation legs in between that used fluidization gas to transport the solid mixture from component to component as shown in Figure 13.

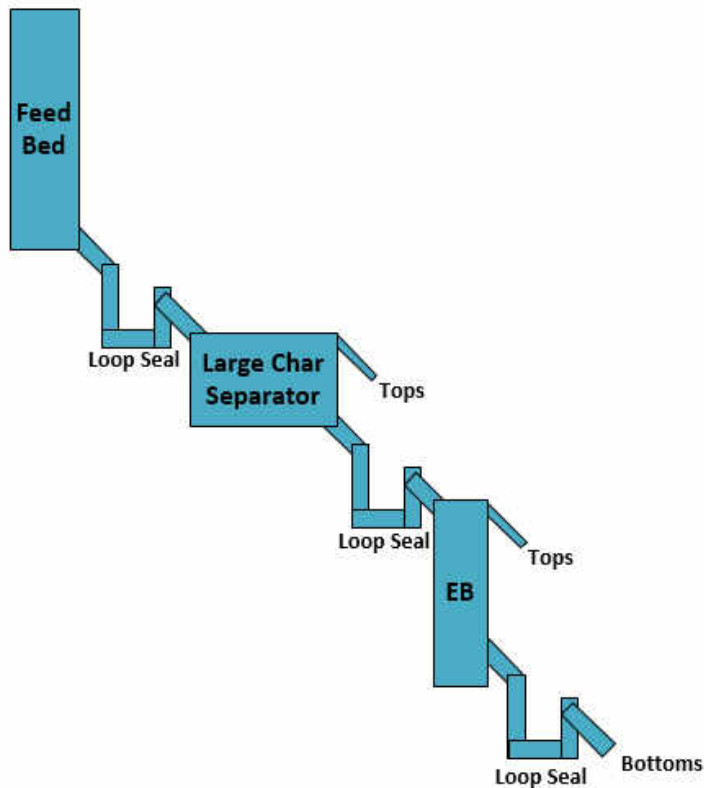


Figure 13: 50kg/hr Char Separation Unit

The LCS system changed from a circular design to a rectangular design in the transition from Phase I to Phase II. OC and char were sourced were from a GE pilot CLC unit. The oxygen carrier of this project consisted of 0.5% char to oxygen carrier by weight. The OC/char Particle Size Distribution (PSD) overlapped in the 150 to 350 μm range as shown in Figure 14.

Initial testing was completed with each individual separation component, before being integrated into a single separation system. The 50 kg/hr char separation tests were continuous, meaning that the solids flow-rate through the system was 50 kg/hr for the duration of the tests. In the LCS, char is segregated and rises to the top of the bed and is subsequently removed. From testing of the LCS under 50 kg/hr operation, there was 77% reduction of char. Figure 14 represents the char removal percentage by size fraction. For these tests, char reduction was determined using a comparison of the char concentration in the bottoms compared to the tops. The LCS performance is quite efficient for char particle sizes below 300µm, having greater than 60% removal in every size fraction smaller than 300µm.

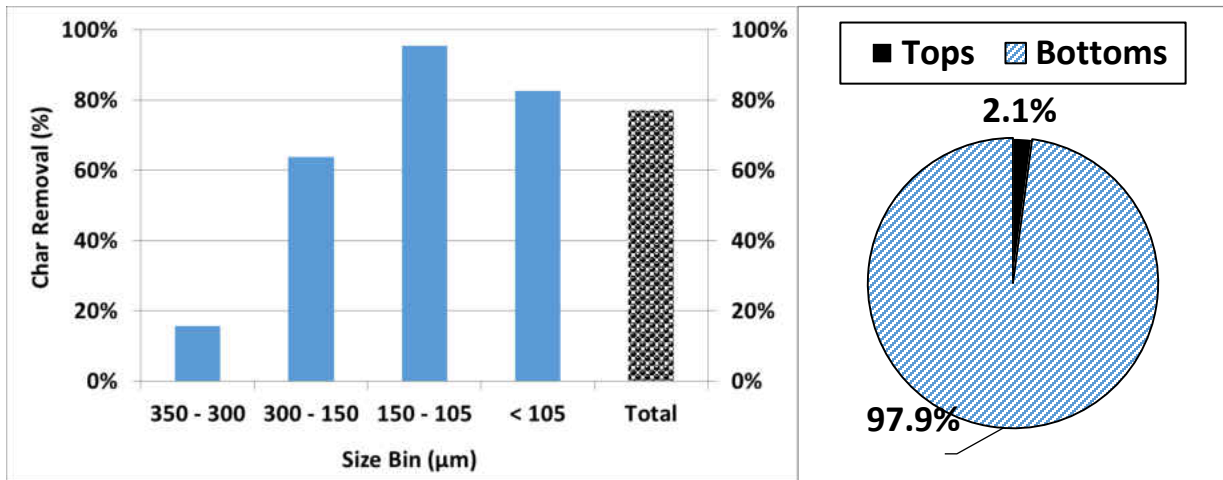


Figure 14: LCS results for 50kg/hr test of 0.5wt% char/OC mix

The char depleted OC from the LCS was then fed into the EB. In the EB, 50 kg/hr test performances removed 22% of the remaining char. As shown in Figure 15 below, EB removed char in mainly the 105-150 µm range. It is important to note that the EB in this experiment was used as a polishing step, as the placement of the EB was located downstream of the LCS. This means some of the char had already been separated out by the LCS before it reached the EB. Placing the EB downstream of the LCS helped lower operational velocities and decrease OC entrainment in the EB.

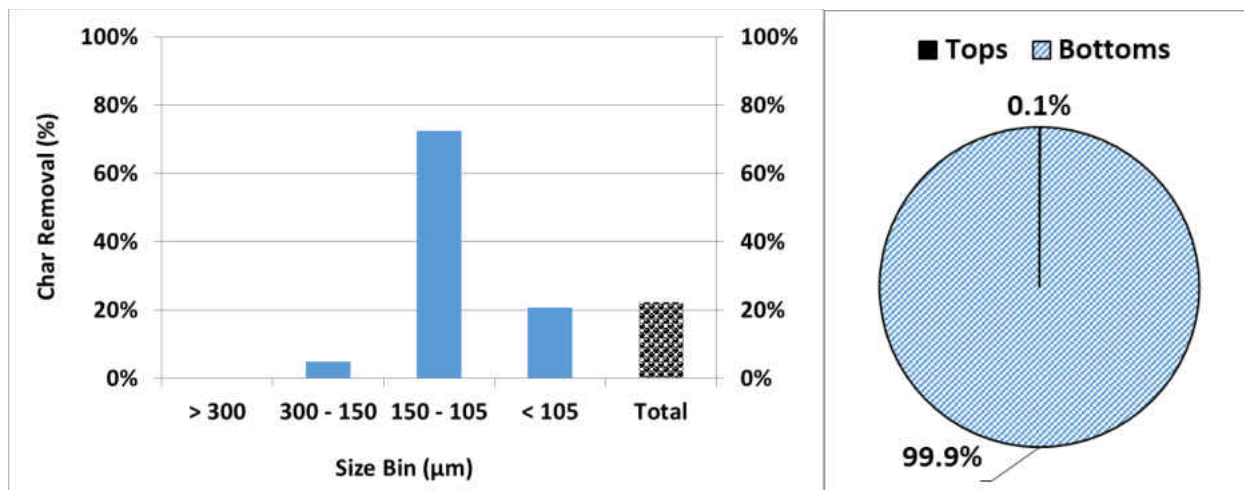


Figure 15: EB results for 50kg/hr test of 0.5wt% char/OC mix

Figure 14 and Figure 15 show that the LCS has an overall better performance of separation than the EB across all size fractions. These results show the LCS to be more efficient at char removal than the EB, which suggests that replacing the EB with the LCS is a possibility if the technology can be developed further. The LCS-EB configuration was identified as the best order for char segregation. This configuration of the LCS with the EB, yielded a combined removal of 82%. The successful results of the scale-up from the lab-scale in Phase I to the 50 kg/hr conditions of Phase II gives validates that this technology may be able to be applied to scaled up CLC systems. This leads into the purpose of this thesis, where the scale-up feasibility of a Char Separation unit at 500 kg/hr (~1000 lb/hr) will be investigated.

The Solution

Following the successful results from Phase II-A-, the feasibility of implementing a carbon stripping technology at higher solid flow rates needed to be explored. This Char Separation Phase II –B– 500 kg/hr project was designed to test whether or not separation results are dependent of scale. This project has strong emphasis on design and fabrication, fluid mechanics/material transport, as well as thermodynamics.

The placement of the char separator in a chemical looping combustion system is shown below in Figure 16. In CLC systems, when unburnt fuel leaves the fuel reactor, combustion of the unreacted fuel (char) occurs inside the air reactor. This causes a release of CO_2 which causes the process in to incur a carbon capture rate penalty. The purpose of this project is to attempt to solve this problem by separating out the char from the oxygen carrier before it is introduced into the air reactor. The char can then be transported back into the fuel reactor to be consumed and produce energy.

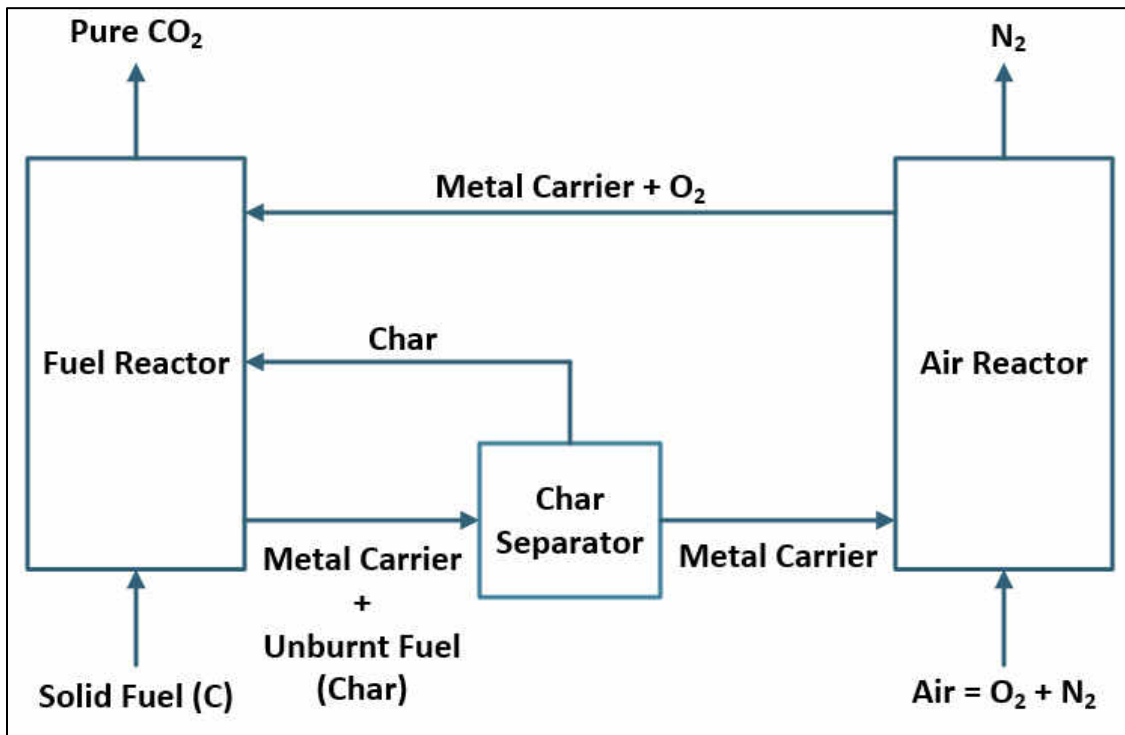


Figure 16: Chemical Looping Combustion Process showing Char Separation

Project Description

The goal of this project is to design, build, test, and report on a char separator. The char is being separated from a solid oxygen carrier. For the purpose of this work, char in this case can be considered as coal/fuel that was not fully utilized after being burned to create energy. The system was designed as a cold-flow unit at 500 kg/hr (~1000 lbs/hr), with intentions to upgrade to a pilot

size hot-flow scale. The focus of this project was on the cold-flow unit only. Cold-flow can be defined as operation at room temperature.

The Char Separation system consisted of multiple sections that were tested individually before being integrated and tested together. The oxygen carrier sourced was in an amount sufficient for testing, (~2000kg). The char concentration in the oxygen carrier was at 0.5-2% weight concentration mixes. An emphasis was placed on using clear/see through materials in order to assist with flow visuals. The oxygen carrier/char mix started in a feed hopper, which was then transported into a large char separator. The goal of the large char separator is to extract the larger size fractions of char into a separate holding vessel. The oxygen carrier at this point was mixed with mostly the smaller size fraction of char. This mix was then transported into an elutriation bed, sometimes referred to as a small char separator (SCS), where the fluidizing air is fast enough to transport the lighter fine char particles out, but not enough to transport the dense oxygen carrier.

The important components of the project are as follows: Large Char Separator (LCS), Small Char Separator (SCS), Hoppers/Feed Beds, Transportation Legs/Loop Seals, and the electronics. Loop seals for solids transport are critical and needed to be designed and calibrated. Loop seals accuracy depend heavily on operating pressures and temperatures. Since the system operated under ambient conditions, these loop seals allowed for simple, consistent flow rates. Pressure transducers and mass flow controllers were used to monitor pressures, have consistent flowrates in every test, along with allowing for a method of verifying operational velocities and minimum fluidization velocities. A Piping and Instrumentation Diagram (P&ID) is provided in Figure 17.

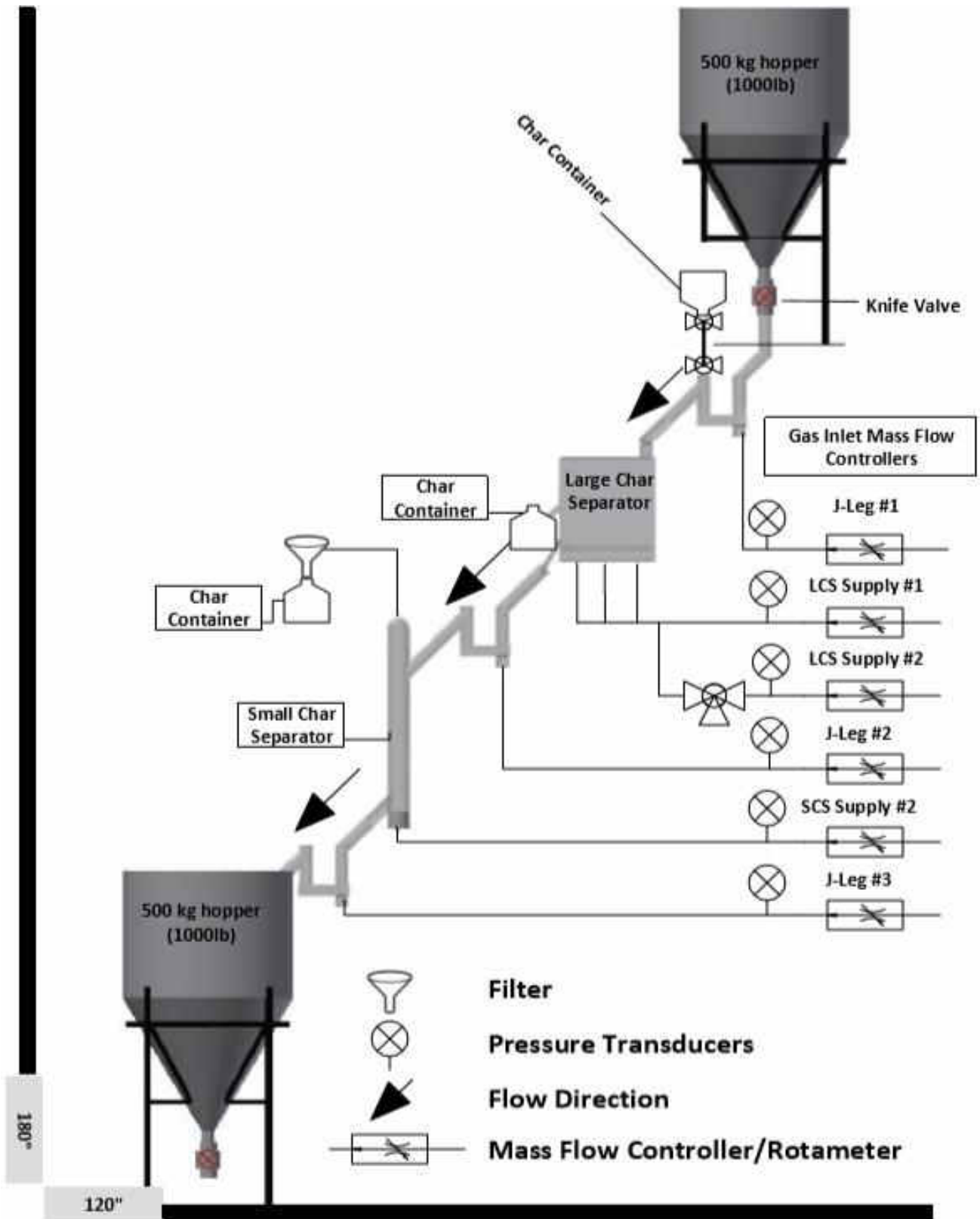


Figure 17: Piping and Instrumentation Diagram

Project Objectives

The goal for this project was to investigate a carbon stripper technology at a flow rate of 500 kg/hr and an increased bed surface area (0.08m^3). An underlying target is set at an 80% reduction of char moving into the air reactor. This is a purity level of 99.8% oxygen carrier. This value is chosen because it minimizes the production of CO_2 from combustion of residuals/carry-over char from the fuel reactor. While removing the char from the oxygen carrier is important, it is also important that the amount of oxygen carrier that is not removed with the char is minimized. This leads to a desired split of 20%. The split is defined as the amount of OC being separated out divided by the total amount of starting OC. The splits will be transferred back into the fuel reactor, so that the char separated out can be fully utilized.

By removing the char from the oxygen carrier and returning it back into the fuel reactor, the system becomes more efficient by production more energy and reducing the required amount of energy needed to capture CO_2 . Another goal is to reduce the residence time needs in the LCS. This is to allow more material to pass through the LCS for any given size, allowing the footprint to be reduced. Priority was placed on investigating the LCS and evaluating the feasibility of the technology at the higher solids flow rate and increased bed surface area. This is in effort to use space efficiently, but also to decrease the total amount of gas/energy required to operate the system.

Scope of this project

For this project a method for char separation from oxygen carriers that is specifically tailored to chemical looping combustion and its unique constraints and process conditions was investigated. The segregation system consists of a novel combination of methodologies that together provide very high segregation efficiency. Following the successful demonstration in Phase I at the lab-scale, this Phase II-B- project involved a significant scale-up, from 50 kg/hour

to 500 kg/hr. The char concentration in both the oxygen carrier and ash mixture is in a range from 0.5% to 2% by weight.

The project strongly emphasized fluidized bed principles in its components. The oxygen carrier/char mix starts in a feed hopper. The mix is then transported into a large char separator (LCS) that is fluidized. The purpose of the large char separator is to extract the larger size fraction of char into a separate holding vessel. The oxygen carrier at this point mostly the smaller size fraction of char. This mix will be transported into another bed contains (small char separator (SCS)) where the fluidizing air is fast enough to transport the lighter fine char particles out of the SCS, but not enough to transport the dense oxygen carrier out into a holding vessel. Loop Seals were employed to aid in the transportation of the mixture and are placed between each component.

As part of this project, the char separation system was designed, built, and tested based on fluidization engineering principles. A key design contribution was a novel loop seal employed to transport solids. Without a loop seal that was specifically tailored for this application, this char separation system would have never become operational. Another contribution was to maximize the visibility of the process by implementing clear components where feasible. An important design factor to be considered was the sealing of the system, as the process involves fine particles. If proper seals were not used, the mixture could leak causing results to be skewed. Additionally, leakage would impact gas flow paths and pressure profiles. This would increase the difficulty in operation and decrease performance.

The key-variables for the testing are gas flow rates within the LCS, SCS, and loop seals, pressures, and solid flow rates. Mass flow controllers were used to control the velocities of the gas and achieve fluidization. Future work will require advanced parametric testing, which is necessary to form relationships between gas and solid flowrates and pressure.

CHAPTER II

EXPERIMENTAL DESIGN & APPROACH

The full assembly was originally intended to be staggered to fit along a staircase; however, the design was slightly altered to be stacked on top of itself in order to optimize floor space. The comparison between staggered and stacked is shown in Figure 18. The actual assembled char separator unit can be seen in Figure 19.

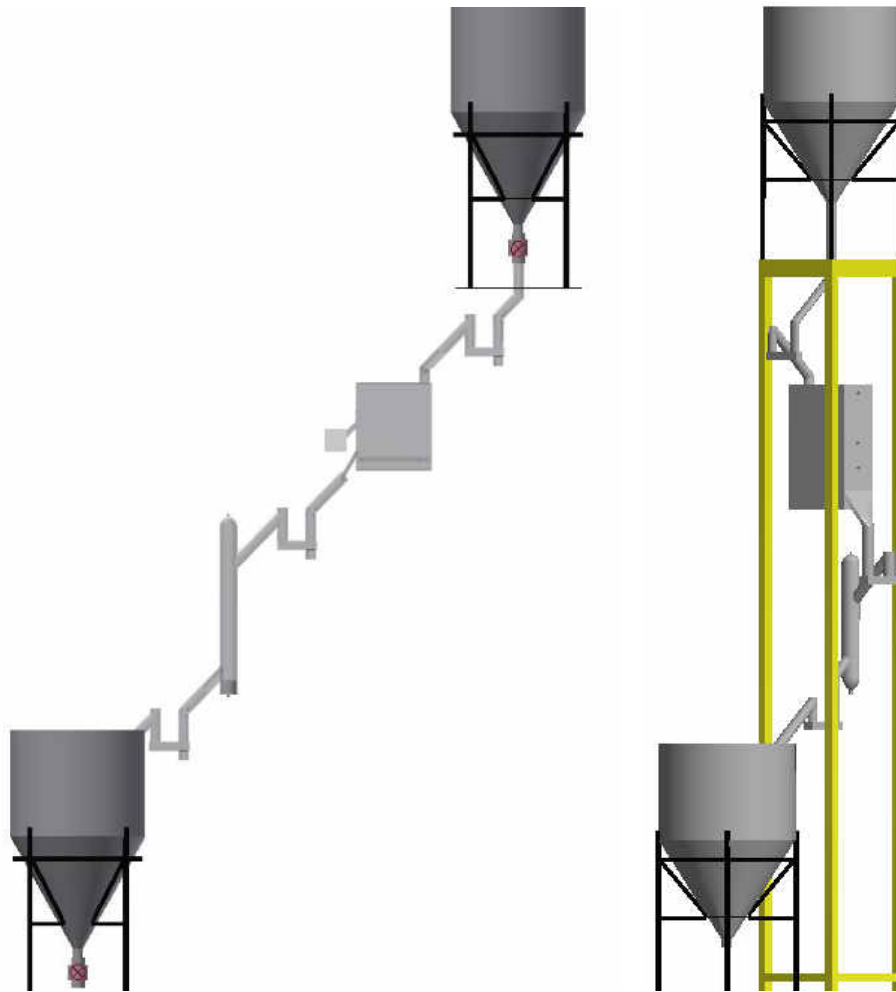


Figure 18: Original Char Separation configuration (Left) Reconfigured Char Separation Unit (Right)



Figure 19: Constructed 500 kg/hr Char Separator

This project consisted of the design and construction of two main components. These components include a large and a small char separator. Between these components are transport legs, which transfer the solid mixture throughout the process. Other components include two large hoppers for storage/feed of the oxygen carrier and two small hoppers for collection of the char. All gases used throughout this experiment were provided through house air. The two OCs used were 94 and 230 microns average particle diameter with a mean density of roughly 2500 kg/m³.

The initial choice of an OC of smaller micron particle was based upon requiring less gas input to fluidize. However, upon testing the finer OC it was found that separation results were poor compared to other previous experiments. Due to these poor results, a new coarse sized OC was sourced and utilized for a comparison. The coarse OC was similar in density, and had an average particle diameter of 230 microns. The carbon/char used had an average particle diameter of 94 microns, with a mean density of 750 kg/m³. Changing from the finer OC to the coarser OC did not cause any re-design to the original equipment other than additional air flow was required. The original design continued to function properly despite the change in OC particle diameter.

Residence Time Analysis

The distributor plate design for the Large Char Separator was one of the most important aspects to ensure the success of this project. There were a variety of factors that were considered when designing the LCS: solids residence time, particle diameter, hole pattern, and discharge heights. The solids residence time is the amount of time that the material stays in the container while being fluidized.

A residence time of 600 seconds was the original design estimation, however, a goal of this project was to reduce the residence time as much as possible in hopes that this would minimize the size of the LCS. A reduction of the size would ultimately lead to less gas input, which is another

goal of this project. To allow residence times to vary, it was necessary to have multiple bed heights/discharge points. This is because the biggest factor affecting residence that can be controlled is the bed volume. In order to have varying residence times for a constant solids throughput without making multiple containers of varying volume, the only variable that could be altered for the volume is the height. Equation 4 is provided for residence time, where the volume is taken into account by the bed weight. Future work can investigate varying the residence times by adjusting the solids feed rate through the loop seal.

$$Residence\ time = \frac{Throughput\ \left(\frac{kg}{hr}\right)}{Bed\ Weight\ (kg)} * \frac{3600s}{hr} \quad (4)$$

The final dimensions for the LCS were 20cm x 40cm x 76 cm. There is a 2.54cm plenum, with char discharge points at 15cm, 30cm, and 60cm (see Figure 20). These discharge points resulted in residence times of 200 seconds, 400 seconds, and 800 second respectively at a solids throughput at 500 kg/hr, as seen in Table 2 below. This gives an optimistic range of potentially successful results based on previous test results, along with the ability of testing the residence times below the 600 second baseline. The distributor plate is made of 1.27cm thick clear polyurethane; the thickness was necessary to support the 100 kilograms of material.

Table 2: LCS Residence Times Based on Varying Bed Discharge Heights

<i>Throughput</i>	(kg/hr)	500	500	500
<i>Width</i>	cm	20	20	20
<i>Length</i>	cm	40	40	40
<i>Discharge Height</i>	cm	15	30	60
<i>Working Volume</i>	cm ³	12000	24000	48000
<i>Weight</i>	kg	25	50	100
<i>Residence Time</i>	Seconds	200	400	800

The design of the Small Char Separator (SCS) was also critical. The design process was very similar to that of the LCS, however the operating conditions were slightly different. The SCS behaves as a fluidized bed. The important factors to consider while designing the SCS were residence time and optimal separation velocity. The residence time calculation is the same as it was for the LCS. The bed height in this stage remains fixed, as this bed is primarily used as a polishing step to take the fine char out of the system that the LCS may have missed. For this reason, the SCS has a shorter residence time goal of 30 seconds. Based on Equation 4, the calculated residence time for the SCS was 32 seconds.

Table 3: SCS Residence Time

<i>Throughput</i>	(kg/hr)	500
<i>Radius</i>	cm	4.45
<i>Bed Height</i>	cm	35.5
<i>Bed Volume</i>	cm ³	2265
<i>Weight</i>	kg	4.5
<i>Residence Time</i>	seconds	32

Large Char Separator Design

The large char separator is the most important component in the char separation system. Its purpose is to separate the larger char particles from the oxygen carrier (ilmenite) using fluidizing gas. The material enters the LCS at the top through a 5.08cm connection coming from a transport leg. Based upon the particle size and density differences between the ilmenite and char, the char will move to the top layer of the fluidized. During this process, oxygen carrier is removed from the bottom of the bed using a loop seal while char is removed from the top of the bed as the bed height reaches the exit port for the char. A picture of the large char separator is shown in Figure 20.

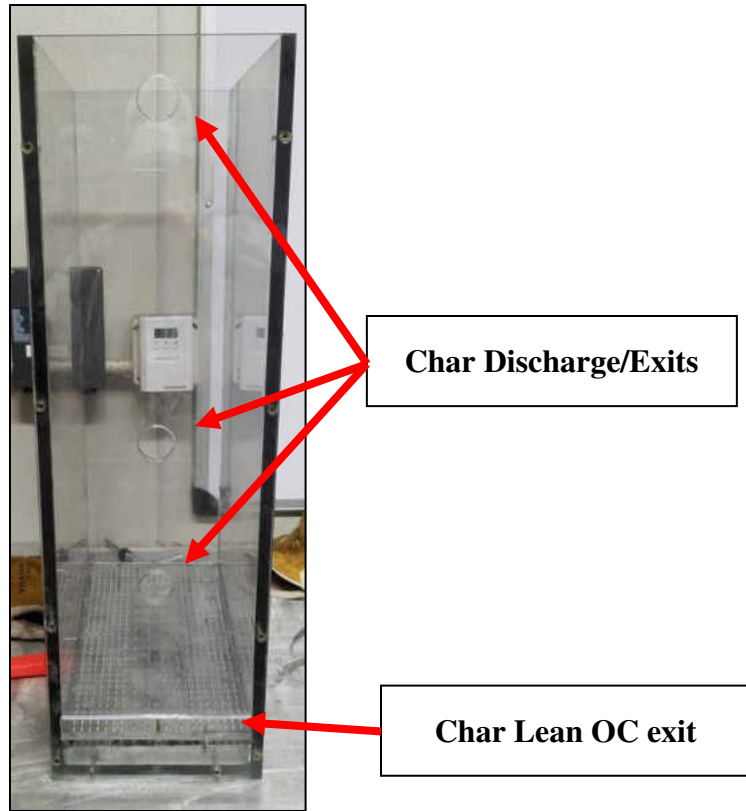


Figure 20: Large Char Separator

The large char separator is a rectangular bed and is 40cm long, 20 cm wide, and 76cm tall. The maximum bed height while operating is 60cm with options to also remove bed material at heights of 15 cm and 30 cm. The rectangular bed is placed on screws that allow the angle to be increased or decreased to help with flow directionality. A vibrator is connected to the LCS to aid in fluidization.

The Distributor Plate

The distributor plate is a key component of the LCS. Airflow was provided via a large compressor and controlled by mass flow controllers, causes the bed to become fluidized. The exact details and method of separation of the oxygen carrier from the char is protected intellectual property. An image of the distributor plate is shown in Figure 21. As shown, there is a pattern on the plate that helps direct the flow of solids to the center. This design assisted in the char removal

by funneling the char to the top and center of the bed in which is then removed from the process via a 2.54cm pipe.



Figure 21: Distributor Plate for Large Char Separator

The pattern was a scaled-up version of the Phase II-A- work, keeping to a two-to-one ratio of length to width. The design was created in AutoCAD Inventor and drilled using the University's CNC machine. The optimal amount of holes as well as pitch was calculated, where pitch refers to the maximum distance between holes to prevent dead zones. In a fully operational system, the existence of dead zones can create hot spots that can lead to sintering and agglomerates of the OC. With little to no risk of the OC sintering or agglomerating, the pitch was not a critical aspect since this is a cold flow design, however, the information was taken into consideration for the final design. Using an average particle size of 94 microns, a hole size of 0.397mm was used to prevent

particles from filling up the plenum and air lines. Since the OC accounts for above 98% of the mixture, operational values were based off of the density of the OC.

Fluidization Engineering Calculations

The process for calculating the estimated minimum fluidization velocity, pitch, and amount of holes is provided below. Since sphericity (ϕ_s) and void fraction in a bed at minimum fluidization conditions (ϵ_{mf}) are not necessarily known, Equation 5 or 6 must be used to solve for minimum fluidization velocity, U_{mf} . Assume that Wen & Yu are referenced for regression values.

$$\frac{d_p u_{mf} \rho_g}{\mu} = \left[28.7^2 + \frac{0.0494(d_p^3 \rho_g (\rho_s - \rho_g) g)}{\mu^2} \right]^{\frac{1}{2}} - 28.7 \quad (5)$$

or

$$Re_{p,mf} = [28.7^2 + 0.494Ar]^{\frac{1}{2}} - 28.7 \quad (6)$$

Where Ar is Archimedes number, defined below in Equation 7. $Re_{p,mf}$ is the Reynolds number which at minimum fluidization velocity, can be used to solve for the minimum fluidization.

$$Ar = \frac{d_p^3 \rho_g (\rho_s - \rho_g) g}{\mu^2} \quad (7)$$

The Reynolds number is directly related to the minimum fluidization velocity by the relationship in Equation 8.

$$Re_{p,mf} = \frac{\rho_g u_{mf} d_p}{\mu_g} \quad (8)$$

U_{mf} can still be estimated by using Equation 9. K_1 and K_2 are referenced regression values, which are provided in Table 4.

$$K_1 Re_{p,mf}^2 + K_2 Re_{p,mf} = Ar \quad (9)$$

Table 4: Regression Values for Calculating Minimum Fluidization Velocity

<i>Investigators</i>	First, $K_2/2K_1$	Second, $1/K_1$
<i>Wen, Yu</i>	33.7	0.0408
<i>Richardson</i>	25.7	0.0365
<i>Saxena and Vogel</i>	25.3	0.0571
<i>Dolomite and hight temperature and pressure, Babu et al.</i>	25.3	0.0651
<i>Correlation of reported data until 1977</i>		
<i>Grace</i>	27.2	0.0408
<i>Chister et al. (Coal, Char, Ballotini (up to 64 bar))</i>	28.7	0.0494
<i>Reference for regression values</i>		
<i>First, $K_2/2K_1$</i>	33.7	
<i>$1/K_1$</i>	0.0408	

Re-arranging Equation 8, U_{mf} can be calculated for as shown in Equation 10. Table 5 provides reference values, the resulting estimated minimum fluidization velocity, and operational flow rate (Q) for the 94 micron OC.

$$u_{mf} = Re_{p,mf} * \mu_g / (\rho_g d_p) \quad (10)$$

Table 5: Reference Values for Calculations – 94 micron OC

<i>Density of gas, ρ_g</i>	1.165	kg/m³
<i>Density of solid, ρ_s</i>	2500	kg/m ³
<i>Mean Particle Diameter, d_p</i>	94	μ m
<i>Viscosity of gas, μ_g</i>	1.76E-05	kg/m.s
<i>Archimedes Number, Ar</i>	211	
<i>Reynolds Number, $Re_{p,mf}$</i>	0.1275	
<i>Minimum Fluidization Velocity, u_{mf}</i>	0.98	cm/s
<i>Operational Flow Rate, $Q_{20^\circ C}$</i>	49	slpm

Table 6 below provides the same information as Table 5, except calculations and values were based of the coarse OC particle, which has a mean particle size of 230 microns.

Table 6: Reference Values for Calculations - 230 micron OC

Density of gas, ρ_g	1.165	kg/m³
<i>Density of solid, ρ_s</i>	2500	kg/m ³
<i>Mean Particle Diameter, d_p</i>	230	μm
<i>Viscosity of gas, μ_g</i>	1.76E-05	kg/m.s
<i>Archimedes Number, Ar</i>	211	
<i>Reynolds Number, $Re_{p,mf}$</i>	0.1275	
<i>Minimum Fluidization Velocity, u_{mf}</i>	4.3	cm/s
<i>Operational Flow Rate, $Q_{20^\circ\text{C}}$</i>	210	slpm

Using Table 5 and Table 6 to compare differences in minimum fluidization and operation flow rates between 94 and 230 micron OC particles, it is estimated that the coarse OC will require a magnitude of 4 times the amount of flow than the finer OC. Since the surface area increase from 94 micron to 230 micron is roughly the same magnitude, this scale is reasonable.

To determine the pitch and required amount of holes in a distributor plate, a several inputs are required: the minimum fluidization velocity, hole size, bed height, bed surface area, and flow rate. Knowing these parameters, the next step in calculating the amount of holes required in the distributor plate is to find the differential pressure across the bed. Equations 11 and 12 display how to calculate the differential pressure across the bed as well as the estimated differential pressure across the distributor plate.

$$\Delta P_{bed} = \rho_s L_{mf} (1 - e) g \quad (11)$$

$$\Delta P_d = 0.3 \Delta P_{bed} \quad (12)$$

With this information, the orifice velocity, U_{or} , can be determined using Equation 11.

$$u_{or} = Cd \sqrt{2\Delta P_d / \rho_g} \quad (13)$$

Using the operating velocity, orifice velocity, and diameter of the orifice, the number of orifices per unit area, N_{or} , can be found:

$$N_{or} = \frac{u_o}{u_{or}} * \frac{4}{\pi d_{or}^2} \quad (14)$$

This can easily be converted to total number of orifices/holes required by multiplying it by the area of the distributor plate. Following through the equations listed above using values provided in Table 7 on the following page, it was found that a recommended minimum of 574 holes were necessary to fluidize the worst-case conditions of a 60cm bed height. The spacing between each of the holes can be found using Equation 13 below.

$$Square\ Pitch = 1/\sqrt{N_{or}} \quad (15)$$

The pitch for a square hole pattern was 1.3cm apart. Values for other pitch orientations are also provided in Table 7. It is worth noting again that this is a cold flow fluidized bed, operating under ambient conditions. Currently pitch is not a critical design factor, because the issue of dead zones is not applicable to the OC being used at room temperature. However, future work is using this design in a CLC process operating at temperatures over 800°C, so pitch and dead zones are still necessary to take into consideration.

Table 7: Distributor Plate Calculation Variables

20cm x 40cm - Distributor Plate		
Operating flow rate	210	SLPM
Area of operation	0.083	m ²
Flow rate in cubic meters per second	3.50E-03	m ³ /s
Design Temperature	23	°C
U_{op}	0.042	m/s

Table 7 cont.

L_{mf}	0.60	m
e_{mf}	0.5	
u_{mf}	0.044	m/s
ρ_s	2500	kg/m ³
ρ_g	1.165	kg/m ³
μ_g	1.76E-05	kg/m.s
d_p	2.30E-04	m
ΔP_{bed}	7358	Pa
ΔP_{distributor}	2207	Pa
C_d	0.8	
u_{or}	49	m/s
d_{or} = 3-8 d_p	3.97E-04	m
N_{or} per square meter	6949	# orifices/m ²
P (Triangular)	0.0129	m
P (Square)	0.0120	m
P (coalescence)	0.0067	m
P (dead zone)	0.4669	m
Total bed area	0.083	m ²
Total number of orifices for area	574	# orifices

Based on the unique hole pattern that directs char to the center, there was a total of 576 holes. It is well known that fluidized bed calculations are approximate. They are to be used only when experimental means of creating a distributor plate to test are difficult, or used to back up experimental values of fluidization. The bed design used was successful with fluidization, thereby validating the fluidization engineering equations used.

Small Char Separator

The Small Char Separator (SCS) has a similar function to that of the Large Char Separator. The purpose of the SCS is to separate out the finer char from the dense oxygen carrier. The way that this works is that the fluidization velocity is set to a value that is lower than the velocity necessary to transport the dense oxygen carrier, but high enough to allow for transport of the less

dense materials – the char. The SCS acts as a polishing step. The maximum theoretically calculated separation flow rate was 132 slpm (0.60 m/s). At flow rates above this, OC will be transported out of the bed, along with the char. The SCS was made to be as clear as possible, while remaining affordable, in order to be able to see the behavior of the char as the experiment runs. The SCS used a -325 mesh screen as the distributor plate. Figure 22 displays the Small Char Separator.

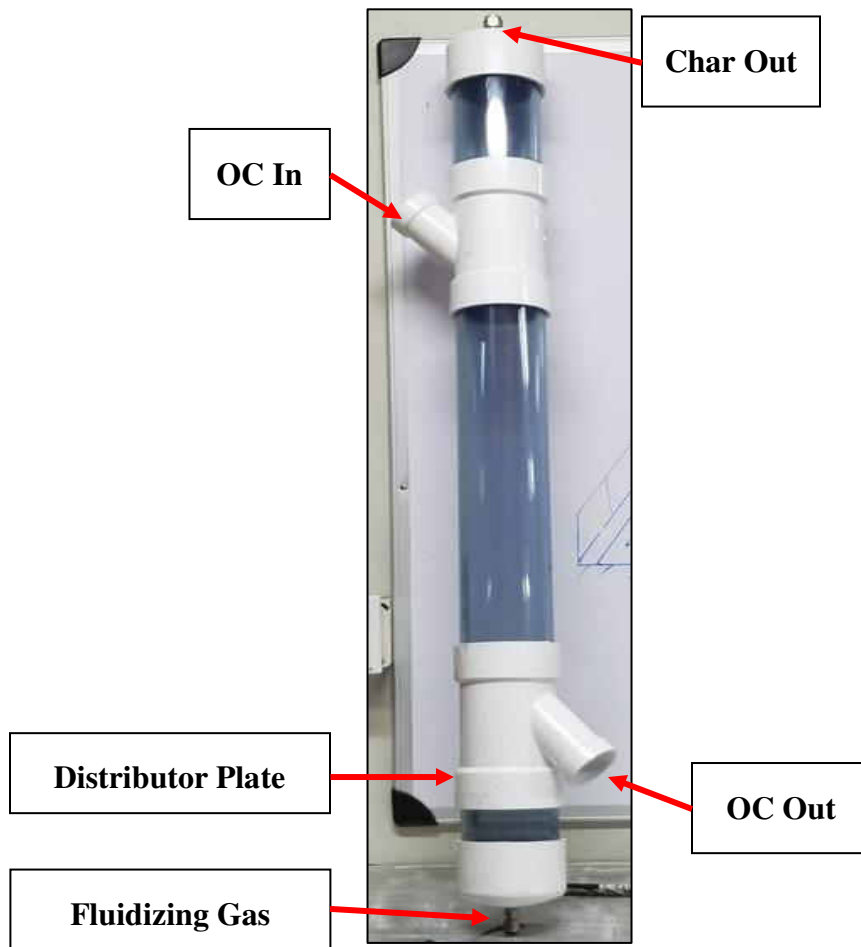


Figure 22: Small Char Separator

One of the more important factors for determining the size of the SCS was the residence time. There was a goal of having a residence time of 30 seconds. With a design feed rate of 500 kg/hr, this was met by using a 4.45cm inner diameter, with a bed height of 35.5cm. This design implemented a 60cm long clear pvc pipe for the midsection to allow enough room for growth of

the bed volume inventory. Since the flowrates were maintained around 500 kg per hour, the SCS needs to be monitored constantly to ensure no backlogging of material occurs. A 0.95cm (3/8”) airline is supplied beneath the bed plenum, which is attached to a rotameter in order to control the gas flow. There is a 1.27cm outlet at the top. As the oxygen carrier-char mixture is transported into the upper left side of the SCS, the lighter particles (char) are then transported up and out to a filter where they can then be collected.

Using a sphericity of 0.8, the terminal velocity of the char can be calculated. The terminal velocity is an important consideration, as the SCS depends on the ability of overcoming the velocity needed to transport the carbon out of the bed while also minimizing the amount of OC that is transported out of the bed. This means the operating bed velocity should be slightly higher than that of the terminal velocity of char, however it should be lower than the terminal velocity of the OC. Making this comparison of velocities will aid in troubleshooting challenges in the SCS if any arise.

$$U_T = \varphi_s \left(\frac{\mu_g (\rho_s - \rho_g) g}{\rho_g^2} \right)^{\frac{1}{3}} \quad (16)$$

The terminal velocity was calculated to be 10 cm/s for char, 34 cm/s for 94 micron OC, and 124 cm/s for 230 micron OC. This yields a smaller range of cut point velocities for the finer OC, while giving a larger range of cut point velocities for the coarse OC.

The optimal separation velocity/flowrate can be determined by using Geldart’s equation for transportation velocity vs minimum fluidization equation, as shown in Equation 17 below [27]. This relationship is used when trying to separate two materials of similar size fractions. The relationship works by finding the optimal velocity for transporting the less dense char, while staying below the transport velocity for moving the bed material.

$$\frac{U_{TO}}{U_{mfs}} = \left(\frac{U_{mfB}}{U_{mfs}}\right)^{1.2} + 0.9 \left(\frac{\rho_h}{\rho_L} - 1\right)^{1.1} \left(\frac{d_h}{d_L}\right)^{0.7} - 2.2 \sqrt{\bar{x} \left(1 - e^{-\frac{H}{D}}\right)^{1.4}} \quad (17)$$

As shown in Table 8 and Table 9, using all the variables listed above yielded an optimal separation velocity of 54 cm/s and 176 cm/s for 94 and 230 micron OC respectively. Converting this velocity to a flowrate is made simple when taking the 3/8" inlet to the SCS into consideration. A calculation for converting a flow velocity to volumetric flowrate is provided below in Equation 18.

$$\begin{aligned} \text{Volumetric Flowrate (Q)} \\ = \text{Flow Velocity (V or U)} * \text{Cross Sectional Area} \end{aligned} \quad (18)$$

Table 8: Separation Cut point Velocity Equation Variables – 94 Micron OC

Minimum fluidization of denser particle (94 micron OC):	$U_{mfB} = 0.983 \frac{cm}{s}$
Minimum fluidization of less denser particle (Char):	$U_{mfs} = 0.452 \frac{cm}{s}$
Density of less dense particle (Char):	$\rho_L = 750 \text{ kg/m}^3$
Density of denser particle (94 micron OC):	$\rho_H = 2500 \text{ kg/m}^3$
Average particle diameters:	$d_H \approx d_L \approx 94 \text{ microns}$
Average concentration of denser particles in mixture:	$\bar{x} = .990099$
Diameter of the fluid bed:	$D = 9.8cm$
Height of the mixture in the fluid bed:	$H = 33cm$
Theoretical separation velocity	$\frac{U_{TO}}{U_{mfs}} = 54 \text{ cm/s}$
Theoretical flow rate	$Q = 41 \text{ SLPM}$

Table 9: Separation Cut point Velocity Equation Variables – 230 Micron OC

Minimum fluidization of denser particle (230 micron OC):	$U_{mfB} = 4.3 \frac{cm}{s}$
Minimum fluidization of less denser particle (Char):	$U_{mfs} = 0.452 \frac{cm}{s}$

Table 9: cont.

<i>Density of less dense particle (Char):</i>	$\rho_L = 750 \text{ kg/m}^3$
<i>Density of denser particle (94 micron OC):</i>	$\rho_H = 2500 \text{ kg/m}^3$
<i>Average particle diameters:</i>	$d_H = 230 \text{ microns}$ $d_L = 101 \text{ microns}$
<i>Average concentration of denser particles in mixture:</i>	$\bar{x} = .990099$
<i>Diameter of the fluid bed:</i>	$D = 9.8 \text{ cm}$
<i>Height of the mixture in the fluid bed:</i>	$H = 33 \text{ cm}$
<i>Theoretical separation velocity</i>	$\frac{U_{TO}}{U_{mfs}} = 176 \text{ cm/s}$
<i>Theoretical flow rate</i>	$Q = 132 \text{ SLPM}$

Transportation Leg/Loop Seal

A novel loop seal was designed and fabricated for moving of solids using a transportation gas. This loop seal differs from the common non-mechanical valves described in the Loop Seals section as it only requires vertical aeration air through the entrance standpipe section. An additional bonus to this design is that the solids exit (weir) is directional, allowing for better directional solids control. The loop seal is comprised of a material entry spout and exit spout, with the transportation gas being applied solely on the material entrance side. Because there are no moving parts, this makes the application of the loop seal ideal for high temperature situations. The operating temperature of the loop seal is only limited by the material used to construct it. The body of the loop seals used in this project was made out of SS304. A distributor screen is utilized to create a uniform flow of gas and to prevent plugging of the gas line.

The loop seal design used for this project was based off of a 2-D schematic of one used in a CFB process, shown in Figure 23. As described earlier, the main differences are that in my design, air flow is only required on one side, not two (see Figure 24Figure 23). Additionally the solids entry and exit are circular pipes instead of rectangular walls.

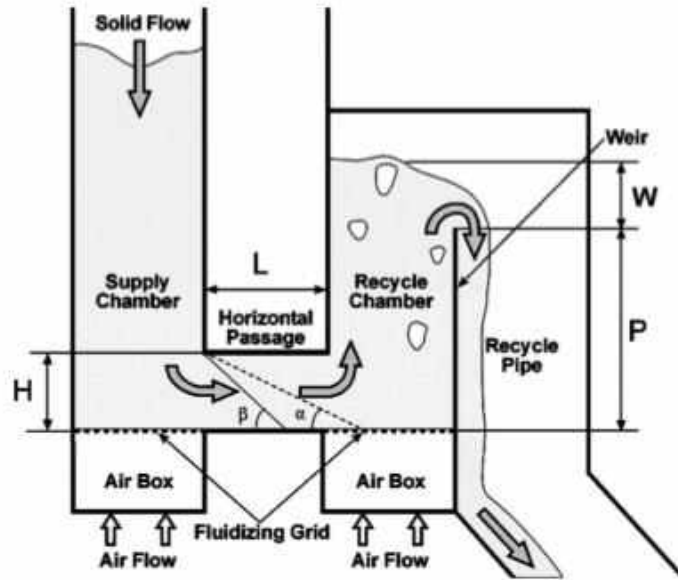


Figure 23: Loop Seal for a CFB Process, Basu et al [28]

Since literature on loop seals and their design is limited, the process for designing the one for this application was completed by trial and error. The entrance and exit are 5 cm pipes. The body was rectangular in shape with an equivalent surface area of the entrance and exit. A 3-D CAD model of the Char Separation Loop Seal design can be seen in Figure 24.

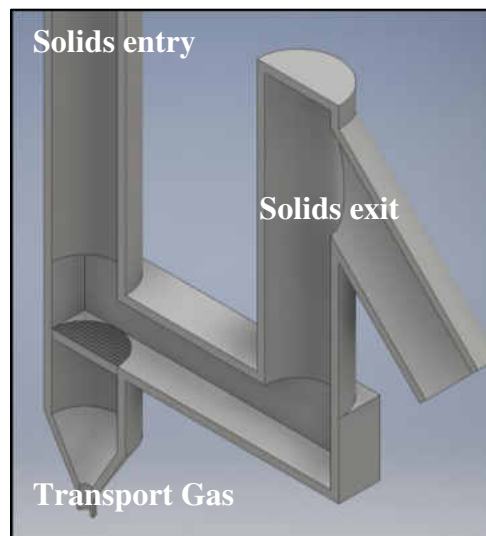


Figure 24: Transportation Leg/ Loop Seal

The amount of material exiting is directly proportional to pressure/ flow rates at the gas entrance. The loop seal entrance requires some solids to maintain a seal, which is determined by

the pressures created by the material between the two spouts. Solid flow rate vs gas flow rate calibration curves are provided for both the fine and coarse OC in Figure 25 and Figure 26. These curves are only an estimate based off measured values. Every loop seal needs to be calibrated individually. For 500 kg/hr solids flow, the resulting gas flow rates were approximately 4.8 SLPM for fine OC, and 21 SLPM for coarse OC.

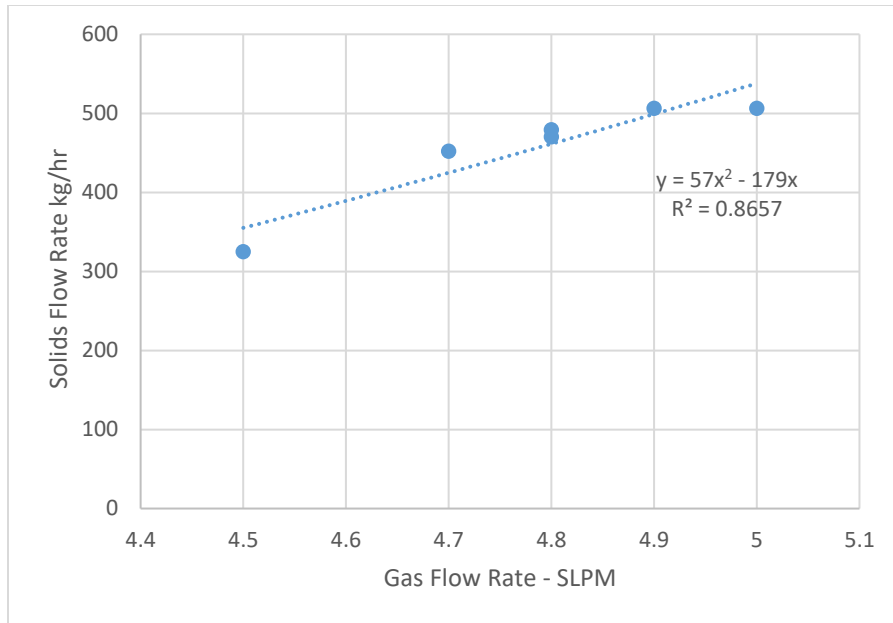


Figure 25: Transport Leg 500 kg/hr Flowrates for Fine OC

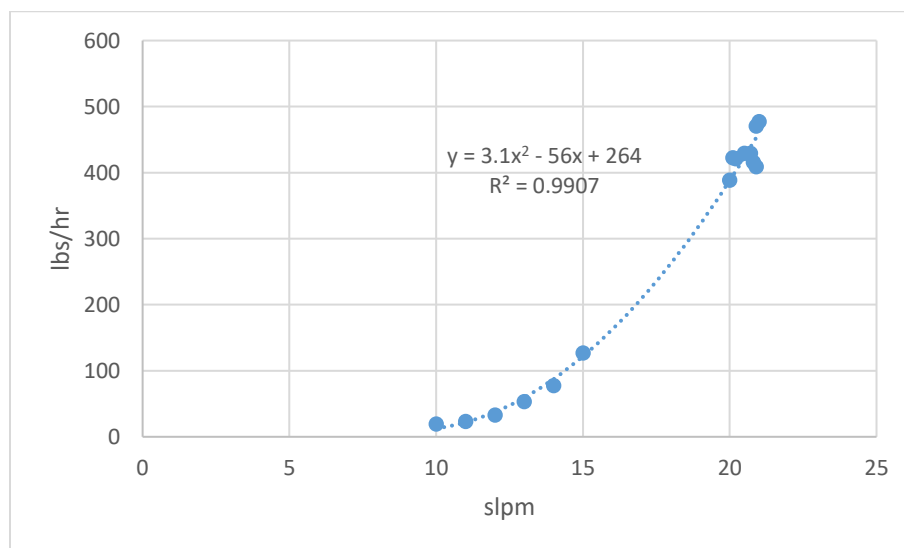


Figure 26: Transport leg 500 kg/hr Flowrates for Coarse OC

Hoppers

Two 85-gallon hoppers are used to store 500 kg of the char/oxygen carrier mixture. They are located at the top as a feed bed, and the bottom as a holding vessel. The two hoppers are exactly the same, which allows for them to be used interchangeably. The 85 gallon hoppers store a total capacity of 850 kg. A crane is available in the project area with a capacity of 2500 kg. This crane, used with two 1000 kg straps, allows for safe lifting of the 500 kg full hoppers when they need to be changed out. The char hopper/separation hopper is of similar design, which incorporates two 7-gallon hoppers. These are capable of storing up to 30 kg of material, which is capable of storing three times the capacity needed for a standard run (e.g. processing 500 kg of material).

Mixing Process

One of the indirect tasks was to develop a method to reliably mix the char with the oxygen carrier. The process chosen needed to promote uniform mixing of the carbon with the OC. For a concentration of 0.5% weight, a total of 5kg of char was required to be mixed with about 500kg of oxygen carrier. A double dump valve system was chosen to automate the process of mixing char into the oxygen carrier as shown below in Figure 27.



Figure 27: Double Dump Valve system set up

Two double dump valves are connected in series with a short section of pipe between them and be controlled via LabVIEW. A 7-gallon storage tank with 5kg of char was mounted above the first valve. The first valve will open to allow a small amount of char into the pipe then it will close. The second valve will open allowing the char to fall into a pipe that is connected to the first transfer leg of the system. Once the char has fallen into the system the second valve will close. Flowrates through this double-dump valve system have proven to be fairly consistent for values between 5-20kg/hr. Two mixing runs total were required, one for each of the 500kg of fine and coarse OCs.

This process relies on the OC material that is moving through the transfer leg to mix the char into the oxygen carrier. It is believed that the fluidizing air that is moving through the transfer leg along with the moving material will be sufficient to mix in the char. The rate at which the char mixes in was tested and calibrated before being implemented. A blow-down line was added to ensure proper feeding through the valve system.

Several random samples were pulled from the resulting mixed char/OC and tested for carbon concentration. Across every test, the carbon concentration was consistent, revealing that this method allowed for homogenous mixing of the char into the OC for a resulting uniform mix.

Holding Structure

The support structure is relatively tall, reaching a maximum of eighteen feet tall. The structure was made of 4.8mm (3/16") thick mild steel square tubing and MIG welded together. An additional two feet was added to the expected total height in order to prevent over constraining the height. The structure is bolted to the ground with cement anchors, as well as welded to the railing for safety purposes.

The structure was originally intended to be staggered downwards following the staircase to allow for ease of access, however it was ultimately decided to put the system in a vertical column

to use the space more efficiently. The hoppers are mechanically fastened to the structure at the top using four ¼” steel threaded rods, with two locking nuts on each rod.

Electronics

The electronics were expensive, but necessary to automate the system and precisely control the flow rates. Implementing electronic control will allow similar operating conditions for each test which should also lead to repeatable results. Three mass flow controllers were used between each component. Using information found from calibrating the transport legs, a correlation between pressure and flowrates of material was made. Using the pressure transducers on every gas input line, in tandem with the mass flow controllers, the flowrates of the solid oxygen carrier-char mixture can be controlled throughout the system. Figure 28 shows an image of the electrical panel.

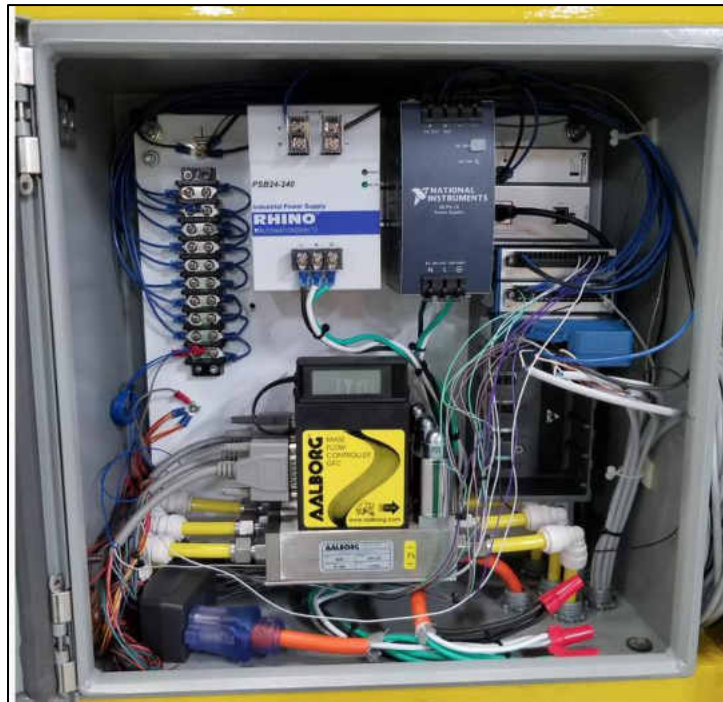


Figure 28: Electronic Panel

In total there are five pressure transducers, three mass flow controllers, and four 24VDC valves. Their location is shown schematically in Figure 17. Each mass flow controller has an output

and feedback. National Instruments technology was utilized, and through LabVIEW, the individual channels can be read, controlled, graphed, and saved.

Programming

Programming and data acquisition from testing the units and assembly were done as a part of this project. This data included pressure measurements, gas flow rates, solid flow rates, and residence times. In order to data-log all the variables, a process control system (PCS) was implemented. The PCS used was LabVIEW 17. An image of the front panel is shown below in Figure 29.

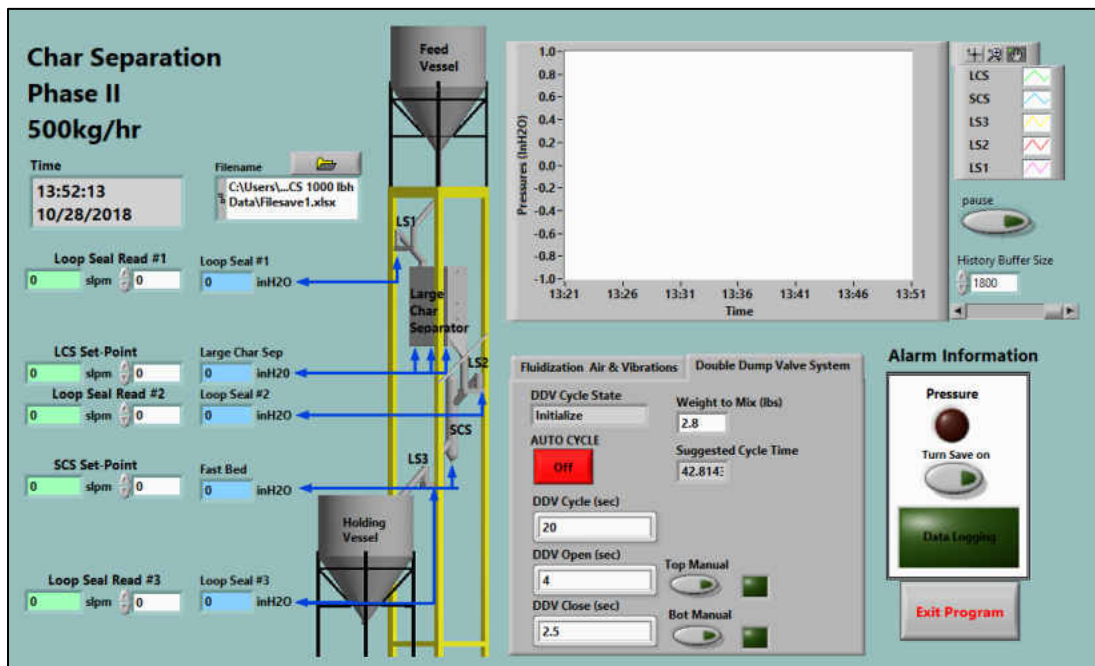


Figure 29: PCS for Char Separation

Although LabVIEW is a visual based programming software, the programming effort was quite extensive. A small portion of the code for this project is available in Figure 30 which helps express the level of coding required to complete this project. This program included controls for mass flow controllers, indicators for flow rates and pressures, double-dump valve controls, graphing, alarms, and a data save.

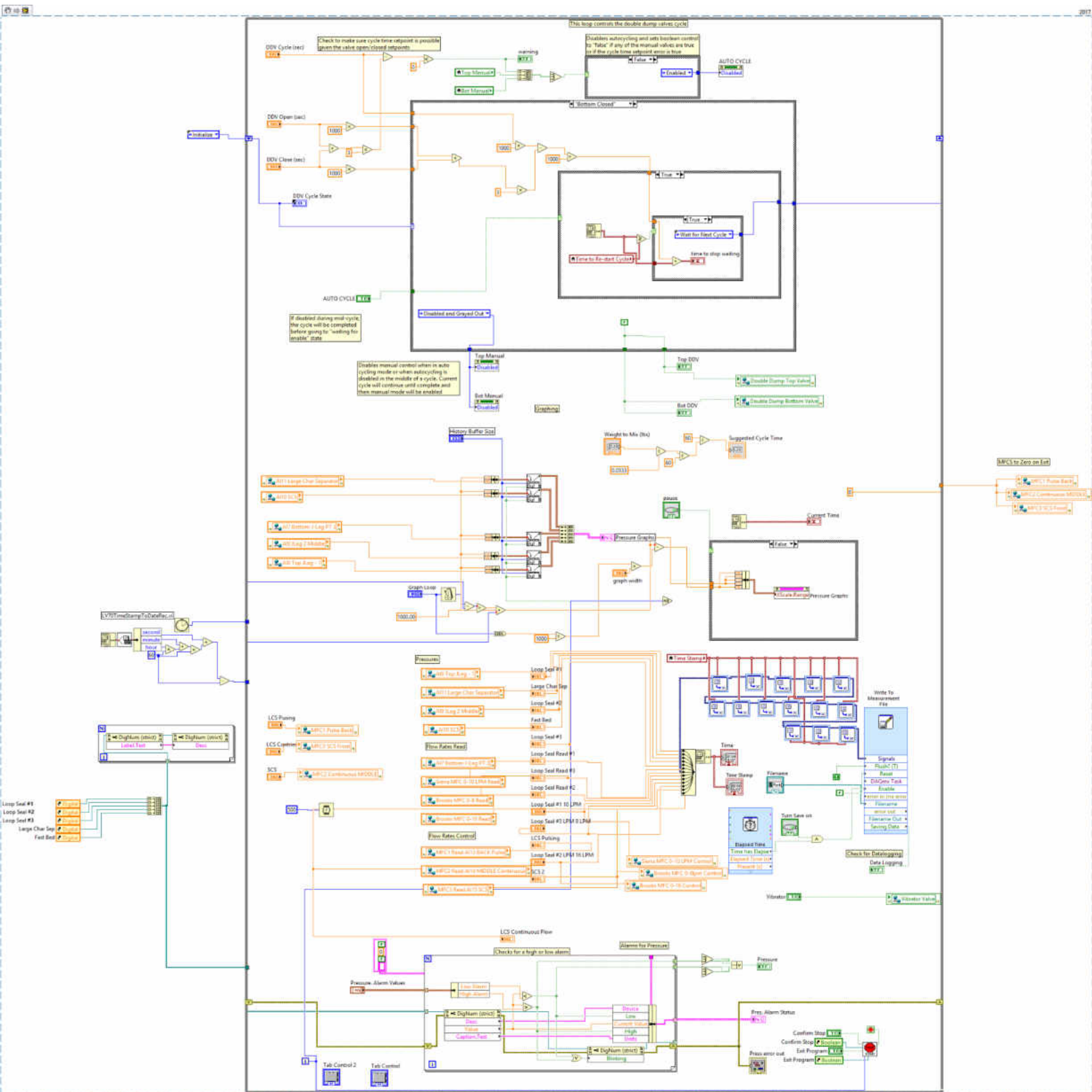


Figure 30: Char Separation - LabVIEW Block Diagram

Approach & Methodology

The two testing methods used in this project were batch testing and continuous testing. Batch can be considered no solid flow rates exiting the beds, or static testing. This type of testing was primarily done to optimize each component individually. Continuous testing would be considered 500 kg/hr entering and leaving the beds. It is worth noting that in relation to an actual CLC system, that this set-up is technically considered a batch system. This is mainly because the storage hopper does not loop back up to the feed hopper in a continuous fashion. All tests were conducted based on average U_{mf} .

Experimentally determining U_{mf}

The core of fluidizing the LCS and SCS is the minimum fluidization velocity for each of the components, for each size of oxygen carrier used. To determine the minimum fluidization velocity, a standard procedure was followed.

1. Fill the bed with char/OC to the operating bed height.
2. Turn on vibrator to aid in fluidization of particles.
3. Apply a flow-rate, incrementally increase the flow at a known small quantity after sufficient time has passed.
4. Measure the pressure at each flow rate and create a pressure vs fluidization velocity curve.
5. Based on the slope on the most linear part of the above curve, the operational U_{mf} can be determined.

Testing Procedure

One of the primary targets was to achieve an average split/recirculation of OC of 20%, meaning 20% of the char/OC mixture is separated out with the char fraction (tops), with the remaining 80% char lean OC exiting the system as bottoms. The split is the ratio of the tops to feeds; with the target being around 20%. Tops refer to char-rich stream that would be recycled to the reducer in the CLC process. Bottoms refer to char-lean stream that feeds the oxidizer. Removal

is the ratio of carbon in the tops to carbon in the feed; with the target being 80%. Each test started with all components as empty of the mixture as possible, to ensure every test was completed with fresh material thereby allowing a direct comparison of results between tests. Fluidization flow rates for the LCS and SCS were set to their respective operating velocities/flow rates.

To help ensure a 20% split, batch runs were conducted. In these batch runs, the bed would be filled at a constant feed rate without any material leaving the bed. The amount of time it took to fill the bed and separation to start would then be multiplied by 20%. Tests were then performed starting with an empty bed. After that 20% time has elapsed, the feed would be shut-off, with the fluidization still remaining on in order to separate and collect the char from the top layer. These tops would then be collected, weighed, and compared to the bottom samples collected. The bottoms samples in these tests were the remaining solids left inside the bed at the end of the test. This procedure would be continued until the entire batch was processed. Using this 20% feed time methodology, I was able to consistently get between 10% and 30% splits. The lack of accuracy on the 20% splits can be attributed to the difficulty of flowing solids. Solids flow are not consistent and vary based on flow rates and pressures of the system. Getting with-in 10% of the 20% splits target was considered satisfactory for these tests.

Combustion testing

Traditional mass balances are an impractical method to determine the separation totals of each of the components because the mixture being separated is not a pure stream of carbon. To analyze the results and find the actual char percentages separated, combustion testing needed to be completed. The mixture that was collected from each test, was separated and split into small sample sizes for testing, around 100 to 1000 grams. Approximately 8kg of material and 35kg of materials for the tops and bottoms respectively. The samples were split using a riffle splitter in

order to have as non-biased representative sample sizes as possible. Combustion testing measures the carbon content by burning the material in a high temp furnace. The volumetric flowrate of CO₂ is determined using from a Laser Gas Analyzer (LGA), and the measured CO₂ is converted into a mass flowrate of carbon.

Method of sample collection

The original method of collecting samples was found to be slightly inefficient part way through testing, skewing the results for the towards higher char concentration in the bottoms. When the bed is emptied, the last layer of char also exits the bed, contaminating the “clean”, bottoms sample and arbitrarily decreases the measured char removal percentage. This means the actual char removal rates are better than they are reported, since the char that normally (in a continuous flow test) would have left the bed with the tops to be separated, is being counted with the exit, bottoms, mixture side. Results should instead compare the “Char in Tops” with “Char Fed” to the unit. For future tests, “Char in Tops” will be compared to “Char in Bottoms” and “Char Fed.” The original testing methodology was continued throughout the remainder of the testing phase in order to have comparable results. Figure 31 represents char left on top of bed that exits into the clean side sample. For continuous testing, the original method of sample extraction is valid, as continuous operation allows for the layer of char that has been separated to remain at the top of the bed, never to travel down and exit.



Figure 31: Char left on top of bed

CHAPTER III

RESULTS & DISCUSSION

Experimentally obtained results of the 500kg/hr large char separation unit will be discussed in this section. Data will also be presented on the scale-up feasibility of this technology. A comparison will be made between the separation efficiency found at 500 kg/hr and previous projects. A ratio of operational velocity to U_{mf} to was used to allow a direct comparison across each of the lower flow-rate scales and oxygen carriers. The results will focus exclusively on operation and performance of the Large Char Separator (LCS).

The resulting measured bed velocities for the Large Char Separator (LCS) and Small Char Separator (SCS) are provided in Table 100. Scale-up is defined by: increasing the feed-rate of solids by 10x, increasing the surface area of the LCS by 1.5x and increasing the surface of the SCS by 1.33x. The experimental velocity was very comparable to the 94 micron size OC, measured 54 cm/s as compared to the theoretical calculated 60 cm/s. Since one focus of the experiment was to reduce gas/energy inputs, the velocity was able to be kept minimized for the 230 micron tests without having significant adverse effects on the separation results.

Table 100: Experimentally obtained optimal bed velocities for 94 to 230 micron particle sizes

	Large Char Separator			Small Char Separator	
Avg. Ilmenite Size (μm)	94 - 230			94 - 230	
Bed Velocity (cm/s)	3 – 10			54	
Bed Dimensions (cm)	20 (W)	40 (L)	15/30/60 (H)	9.8 (diameter)	61 (H)

94 Micron OC Separation Results

It was proven that separation targets were unable to be met for the finer 94 micron ilmenite,. This can be attributed to low U_{mf} of the fine OC, 0.983 cm/s; compared to the U_{mf} of AC \approx 0.45 cm/s. Although this meant a lower flowrate of gas was required to fluidize the bed, it also meant that the separation of particles of the bed suffered due to the bed now being in more of a well fluidized and well mixed regime. Results of char separation throughout a variety of tests are provided for the 94 micron OC in Figure 32. These separation results are for the LCS only. The average U_{mf} is unitless and is based off the ratio of operational velocity to the minimum fluidization velocity for the fine and coarse OC. Several different fluidization regimes were used; A, B, and a combination of the two: AB. The specifics of the fluidization regimes used is intellectual property.

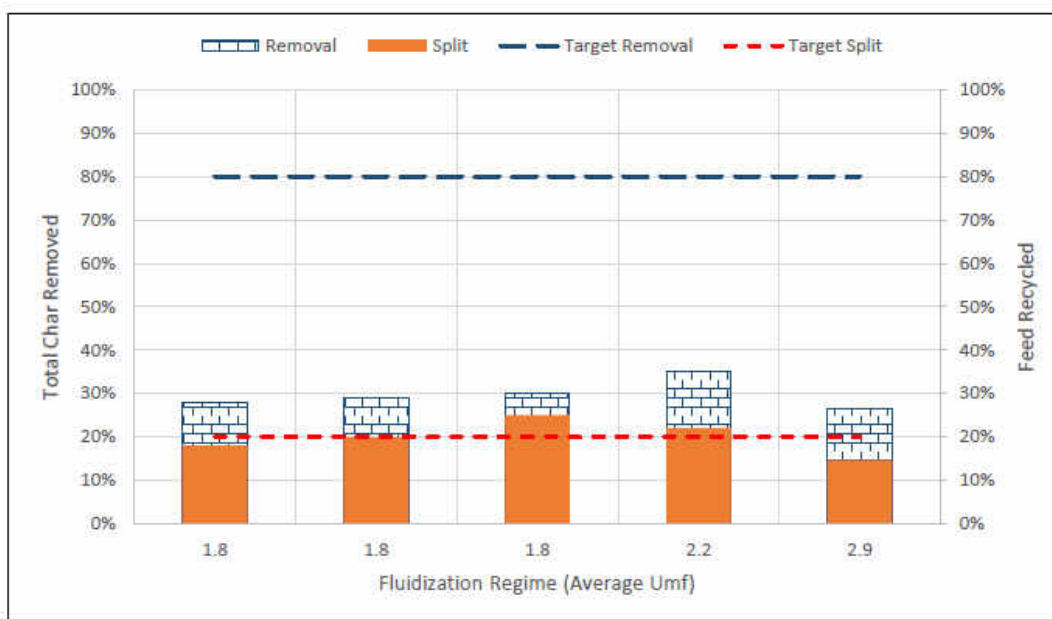


Figure 32: Effect of Flow Regime on 94 μ m OC – All Regime A

Results show that while maintaining a consistent split in the range of 15-25%, the total char removed never exceeded 40%. This fell considerably shorter of the target 80% separation. The average U_{mf} was increased in attempts to increase the amount of char removed. However, it was

revealed that increasing the U_{mf} did not have any significant effects on the total char removed. The total char removed did not increase with additional air, rather, it decreased slightly. These results indicate that increasing the U_{mf} / flowrates beyond a certain point provides no benefits to removing char. This means the fine OC separation performance is relatively insensitive to changes in velocities and that the separation performance of the fine OC is not limited by the amount of gas flow/velocity provided to the bed. Test results for fluidization regimes B and AB performed significantly worse, for this reason efforts were placed on maximizing the operation of fluidization regime A.

Figure 33 represents a comparison of a poor fluidization regime and the method of separation/optimal fluidization regime. This is a top view looking downward at the top layer of the LCS. Even though the distributor plate has a pattern that should guide char to the center, the char does not flow to the center, under the poor fluidization regime, however, it can be seen that for the optimized design the char collects in the center, facilitating easy removal from the bed. This demonstrates that with a proper separation technique, fluidization regime, and distributor plate design, efficient separation of the char is possible.



Figure 33: Poor Fluidization Regime (left) vs Optimal Fluidization Regime (Right) – 94 micron OC

It was found through testing that the impact of solids residence time on char separation for the SCS is negligible, as any of the finer char particles that enter the bed are immediately discharged by the high gas velocity. The significance of this means that the mixture entering the SCS does not need to remain inside the SCS for any extended period of time. The important principle of the SCS was found to be the high operating velocity, which further promotes separation of the char from the dense OC.

To improve the separation of the char from the fine OC, different test conditions and/or distributor plate configurations should be explored. Additional tests can be ran at varying bed heights, which may allow for easier separation of char from the fine OC. Another variable that can be altered is testing of the SCS in jet vs mesh modes, meaning that the SCS grid plate would be redesigned to use a distributor plate with jet holes in it rather than a mesh screen. This would theoretically increase local velocities inside the SCS and promote better transport of the char particles out of the bed.

230 Micron OC Separation Results

After running a variety of tests with the finer OC, it was ultimately decided to switch back to the 230 micron OC. This was done to verify that the poor performance for the fine OC case was based on the particle size and not the behavior of the OC itself. This change in particule size helped increase the char removed by nearly double, averaging around 66% char removal. The splits were comparable to the fine OC, with an average between 10-30%. The 230 micron OC yielded better separation results with a lower ratio of operational velocity to average minimum fluidization velocity than the 94 micron OC. Increasing the operational velocity seemed to have a negative effect on the char removal percentage. The higher operating velocity ultimately leads to better mixing in the bed rather than promoting density driven separation. Overall separation results for

0.8 to 1.0 average U_{mf} proved very consistent. Separation results and feed recycled are shown in Figure 34.

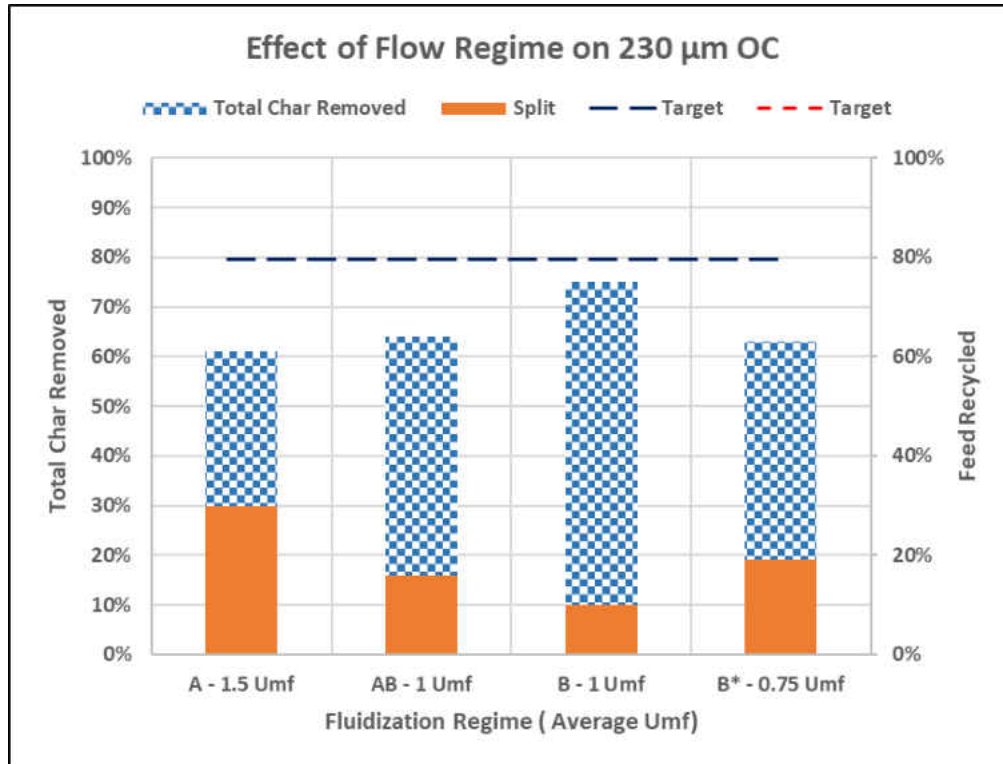


Figure 34: Effect of Flow Regime on 230 μ m OC

Testing of the LCS alone did not meet the target of 80% separation. The best result was found using fluidization regime B, which had a separation of 75% with only 10% splits. Use of fluidization B is promising; where improving the split should improve the char separation. Under the assumption of removing more of the bulk solids increases total char removal, the separation results should also see a slight increase when increasing from a 10% split to a 20% split. With intentions of combining the SCS with the LCS, along with improving the method of sample collection and analyses, it is still very promising that 80% separation of char is achievable. Additional factors that still need to be investigated are bed angle, increase/decreased residence times, solid flow rates, and additional fluidization regimes. Taking these factors into consideration offer a compelling argument of the scale-up feasibility of the LCS/Char Separation system.

Solid Flow-Rate (Scale) vs Separation

The char separation results are compiled for the previous projects, for both fine and coarse oxygen carriers, in Table 11. The previous projects consist of: the Phase I proof of concept, 50 kg/hr; hot and cold, and the 500 kg/hr.

Table 11: Separation Results and Operating Velocities at varying scale and process conditions

Separation Data – Char Removal	Phase I – Proof of Concept	50 kg/hr Fine – Hot flow ~300°C	500 kg/hr Fine – Cold Flow	50 kg/hr Coarse – Cold Flow	50 kg/hr Coarse – Hot flow ~300°C	500 kg/hr Coarse – Cold Flow
LCS	30%	-	35%	77%	-	75%
EB/SCS	43%	-	0%	22%	-	0%
Combined	71%	81%	35%	81%	66%	75%
Splits	29%	43%	22%	2%	19%	10%
Average U_{mf}	-	A: 2.6 U_{mf}	A: 2.2 U_{mf}	AB: .75 U_{mf}	AB: 1.0 U_{mf}	B: 1.0 U_{mf}

In this table, the 500kg/hr separation results are compared to the smaller scales based on separation results and the ratio of U_{op} to U_{mf} . This comparison shows that the coarse OC has on average better char separation with lower splits than the fine OC for the 50kg and 500 kg/hr tests.

The 50 kg/hr fine OC had 81% separation with 43% splits, while the 500 kg/hr had 35% separation and 22% splits. It is reasonable to assume that if the 50 kg/hr splits had a reduction in splits of 50% down to ~22% splits, that the impact it would have on separation would be similar (~ 40% separation). Therefore the char separation results between fine OC for the hot flow and 500 kg/hr are comparable.

The 500 kg/hr unit had comparable separation to that of the 50kg cold flow, but improved separation over the 50kg hot flow. This is attributed to the increased control and operation of the cold flow systems, which operation is aided by being able to visualize the flow. The 50 kg/hr cold flow had 80% less splits than the 500 kg/hr project. This can be credited to slower flow rates in the LCS which allowed improved control over the splits.

CHAPTER IV

CONCLUSION

Chemical Looping Combustion systems are very complex, but offer an alternative method of energy production with the added benefit of carbon capture. CLC systems can be designed in such a manner that the energy losses of the overall process are minimized, while allowing for the separation of the undesired products (e.g., CO₂) produced from the reactions to be easily accomplished. Two main key challenges associated with CLC systems are the high cost of electricity produced from CLC and a carbon penalty resulting from carbon reaching the air reactor. While the high cost of electricity can be lowered by developing lower cost oxygen carriers, the carbon penalty needs to be addressed. Implementing a low energy in-line carbon stripping technology would make CLC a more viable method of energy production.

This project designed, fabricated, built, and started basic tests on a 500 kg/hr char separator for use in a CLC system. A novel loop seal design was developed and utilized throughout this project. While the overall design is the main focus of this thesis, the scale-up feasibility of this technology was the primary goal. Fluidization engineering principles were used to design the core component, the Large Char Separator (LCS) and its distributor plate. Fluidization principles were also used to estimate the operational flowrates and velocities for the Elutriation Bed (EB).

The results demonstrate the LCS ability to separate char, with an average of 30% char

separation with 15-25% splits for a fine oxygen carrier mixture. There was an average of 66% char separation with 15-25% splits for a coarse oxygen carrier mixture. Although these two oxygen carriers fell short of the underlying goal of 80% separation, this target is reasonably feasible with further separation expected in the EB. There are a variety of parametric tests that can still be done to optimize the LCS and char separation system to meet the 80% goal. These tests include using additional size fractions of oxygen carrier, increasing residence times, flow regimes, altering the bed angle, narrowing down on the splits, and implementing/optimizing the EB. Through the testing of the factors listed above, an 80% removal of carbon from the system is a very reasonable.

CHAPTER V

FUTURE WORK

Future work, outside the scope of this thesis, will involve the conceptual level engineering design of pilot-scale char separation systems (~5,000 and 150,000 kg/hr solids throughput) integrated within an actual CLC process. For the purposes of this project, the GE Power CLC pilot systems (100 kWth and 3 MWth) would be used as the boundary condition. This task will include the preparation of process flow diagrams (PFDs), piping & instrumentation diagrams (P&IDs), as well as an equipment specification list and description of the connections/retrofit to the existing pilot system. Key specifications will include items such as: solids flows, residence times, gas flows, gas velocities, temperatures, pressure drops, loop seal designs, and equipment dimensions/geometries. This task will be the basis for future development of the char separation technology in which the pilot system would require a detailed engineering design, construction and testing within an actual CLC process. Following the project, opportunities with GE Power, DOE, and/or others will be pursued to implement such a project.

Planned Work

This technology could also potentially be used to separate char from ash. Future work stemming from this project could involve the scale-up feasibility of separation of inorganic species from recycled char in gasification systems and a novel method of separation of carbon from coal-fired plant ash to generate material to replace cement in concrete. Other applications include

the recovery of coal and valuable rare earth minerals from coal cleaning reject streams; and in post-consumer goods recycling/waste-to-energy based on fragmentation and separation. Separation of char from ash will use similar methodology than the char separation from an oxygen carrier. The properties of the mixture are similar to that of the oxygen carrier mixture. The ash is the bulk solid in this case with a similar weight percentage of char needed to be separated out. The ash is denser than the char by a factor of around 2. However, with the difference in the densities being reduced, the design and testing procedures become a critical aspect to the technology. Controlling the solids flow rates and containment would be a crucial aspect to the success of this technology.

Additional testing can be done with varying conditions to improve separation of fine OC.. If the LCS is able to reach 80% separation with under 20% splits, then a SCS will not be required. More tests will be conducted with the SCS to improve efficiencies, which may answer if the increased benefits of the SCS is enough to warrant the added cost of including the SCS. Further experiments and alterations can be made to the LCS or char separation process in order to potentially improve overall separation results. This would include a variety of tests using the following variables: residence times, solid flow rates, splits, fluidization flow rates & regimes, bed angle.

REFERENCES

- [1] B. Moghtaderi, "Review of the recent chemical looping process developments for novel energy and fuel applications," in *Energy and Fuels*, 2012.
- [2] S. R. e. a. NETL, "Guidance for NETL's Oxy-combustion R&D Program: Chemical Looping Combustion Reference," DOE-NETL Report 2014/1643, 2014.
- [3] C. Linderholm and A. Lyngfelt, "Chemical-looping combustion of solid fuels," in *Calcium and Chemical Looping Technology for Power Generation and Carbon Dioxide (CO₂) Capture*, Elsevier, 2015, pp. 299-326.
- [4] S. Y. Chuang, J. S. Dennis, A. N. Hayhurst and S. A. Scott, "Development and performance of Cu-based oxygen carriers for chemical-looping combustion," *Combustion and Flame*, vol. 154, no. 1, pp. 109 - 121, 2008.
- [5] C. R. Forero, P. Gayán, F. García-Labiano, L. F. de Diego, A. Abad and J. Adánez, "High temperature behaviour of a CuO/ γ -Al₂O₃ oxygen carrier for chemical-looping combustion," *International Journal of Greenhouse Gas Control*, vol. 5, no. 4, pp. 659 - 667, 2011.
- [6] J. Adánez, F. García-Labiano, L. F. De Diego, P. Gayán, J. Celaya and A. Abad, "Nickel-copper oxygen carriers to reach zero CO and H₂ emissions in chemical-looping combustion," in *Industrial and Engineering Chemistry Research*, 2006.
- [7] NETL, "DOE/NETL Advanced Combustion Systems Chemical Looping Summary," U.S. Department of Energy, July 2013.
- [8] S. C. Bayham, H. R. Kim, D. Wang, A. Tong, L. Zeng, O. McGiveron, M. V. Kathe, E. Chung, W. Wang, A. Wang, A. Majumder and L.-S. Fan, "Iron-Based Coal Direct Chemical Looping Combustion Process: 200-h Continuous Operation of a 25-kWth Subpilot Unit," *Energy & Fuels*, vol. 27, no. 3, pp. 1347-1356, 2013.
- [9] H. Leion, T. Mattisson and A. Lyngfelt, "The use of petroleum coke as fuel in chemical-looping combustion," *Fuel*, 2007.
- [10] L. Shen, J. Wu, J. Xiao, Q. Song and R. Xiao, "Chemical-Looping Combustion of Biomass in a 10 kW th Reactor with Iron Oxide As an Oxygen Carrier," *Energy & Fuels*, 2009.
- [11] N. Berguerand and A. Lyngfelt, "Design and operation of a 10kWth chemical-looping combustor for solid fuels – Testing with South African coal," *Fuel*, vol. 87, no. 12, pp. 2713 - 2726, 2008.
- [12] N. Berguerand and A. Lyngfelt, "The use of petroleum coke as fuel in a 10 kWth chemical-looping combustor," *International Journal of Greenhouse Gas Control*, 2008.

- [13] A. Thon, M. Kramp, E.-U. Hartge, S. Heinrich and J. Werther, "Operational experience with a system of coupled fluidized beds for chemical looping combustion of solid fuels using ilmenite as oxygen carrier," *Applied Energy*, vol. 118, pp. 309 - 317, 2014.
- [14] P. Markström, C. Linderholm and A. Lyngfelt, "Operation of a 100kW chemical-looping combustor with Mexican petroleum coke and Cerrejón coal," *Applied Energy*, 2014.
- [15] H. E. Andrus Jr., J. H. Chiu, P. R. Thibeault and A. Brautsch, "ALSTOM's calcium oxide chemical looping combustion coal power technology development.," *International Technical Conference on Clean Coal and Fuel Systems*, 2009.
- [16] T. Mattisson, M. Johansson and A. Lyngfelt, "CO₂ capture from coal combustion using chemical-looping combustion - Reactivity investigation of Fe, Ni and Mn based oxygen carriers using syngas.," *Proceedings of the International Technical Conference on Coal Utilization & Fuel Systems*, 2006.
- [17] M. Johansson, T. Mattisson and A. Lyngfelt, "Comparison of oxygen carriers for Chemical-Looping combustion," *Thermal Science*, 2006.
- [18] A. Abad, T. Mattisson, A. Lyngfelt and M. Rydén, "Chemical-looping combustion in a 300 W continuously operating reactor system using a manganese-based oxygen carrier," *Fuel*, 2006.
- [19] M. Arjmand, H. Leion, T. Mattisson and A. Lyngfelt, "Investigation of different manganese ores as oxygen carriers in chemical-looping combustion (CLC) for solid fuels," *Applied Energy*, vol. 113, pp. 1883 - 1894, 2014.
- [20] M. Kramp, A. Thon, E.-U. Hartge, S. Heinrich and J. Werther, "The Role of Attrition and Solids Recovery in a Chemical Looping Combustion Process," *Oil & Gas Science and Technology – Revue d'IFP Energies nouvelles*, vol. 66, no. 2, pp. 277-290, 2 3 2011.
- [21] K. Mayer, E. Schanz, T. Pröll and H. Hofbauer, "Performance of an iron based oxygen carrier in a 120 kWth chemical looping combustion pilot plant," *Fuel*, vol. 217, pp. 561 - 569, 2018.
- [22] D. Kunii and O. Levenspiel, "{CHAPTER} 3 - Fluidization and Mapping of Regimes," in *Fluidization Engineering (Second Edition)*, Second Edition ed., D. Kunii and O. Levenspiel, Eds., Boston, Butterworth-Heinemann, 1991, pp. 61 - 94.
- [23] D. KUNII and O. LEVENSPIEL, "ENTRAPMENT AND ELUTRIATION FROM FLUIDIZED BEDS," *Journal of Chemical Engineering of Japan*, vol. 2, no. 1, pp. 84-88, 1969.
- [24] Y. O. Chong, D. P. O'Dea, L. S. Leung, D. J. Nicklin and J. Lottes, "{DESIGN} {OF} {STANDPIPE} {AND} NON-MECHANICAL V {VALVE} {FOR} A {CIRCULATING} {FLUIDIZED} {BED}," in *Circulating Fluidized Bed Technology*, ed., P. Basu and J. F. Large, Eds., , Pergamon, 1988, pp. 493 - 500.
- [25] T. Knowlten, "Nonmechanical Control of Solids Flow in Chemical Looping Systems," in *NETL 2011 Workshop on Multiphase Flow Science*, Pittsburgh, 2011.
- [26] M. Kramp, A. Thon, E. U. Hartge, S. Heinrich and J. Werther, "Carbon Stripping - A Critical Process Step in Chemical Looping Combustion of Solid Fuels," *Chemical Engineering and Technology*, 2012.

- [27] D. Geldart, "Chapter t - Solids Mixing," in Gas Fluidization Technology, UMI, 1998, p. 113.
- [28] P. Basu and J. Butler, "Studies on the operation of loop-seal in circulating fluidized bed boilers," Applied Energy, vol. 86, no. 9, pp. 1723 - 1731, 2009.
- [29] T. A. B. C. D. C. S. Y. C. J. P. E. S. S. A. D. J. S. Müller C. R. and Brown, "Experimental Investigation of Two Modified Chemicallooping Combustion Cycles Using Syngas from Cylinders and the Gasification of Solid Fuels," in Proceedings of the 20th International Conference on Fluidized Bed Combustion, Berlin, Heidelberg, 2010.
- [30] A. Lyngfelt, "Chemical-looping combustion of solid fuels – Status of development," Applied Energy, vol. 113, pp. 1869 - 1873, 2014.
- [31] T. Dixon, K. Yamaji, A. Lyngfelt, P. Markström and C. Linderholm, "Chemical-Looping Combustion of Solid Fuels — Operational Experiences in 100kW Dual Circulating Fluidized Bed System," Energy Procedia, 2013.
- [32] J. Bao, Z. Li and N. Cai, "Experiments of char particle segregation effect on the gas conversion behavior in the fuel reactor for chemical looping combustion," Applied Energy, vol. 113, pp. 1874 - 1882, 2014.
- [33] J. Adánez, F. García-Labiano, L. F. de Diego, P. Gayán, J. Celaya and A. Abad, "Nickel–Copper Oxygen Carriers To Reach Zero CO and H₂ Emissions in Chemical-Looping Combustion," Industrial & Engineering Chemistry Research, vol. 45, no. 8, pp. 2617-2625, 2006.
- [34] J. Andrus Herbert E. [Alstom Power Inc. Windsor CT (United States)], J. H. [P. I. Chiu Windsor CT (United States)], C. D. [P. I. Edberg Windsor CT (United States)], P. R. [P. I. Thibeault Windsor CT (United States)] and D. G. [P. I. Turek Windsor CT (United States)], "Alstom's Chemical Looping Combustion Prototype for CO₂ Capture from Existing Pulverized Coal-Fired Power Plants," , United States, 2012.